DCT 195

Load Rating of Bridges Without Plans

by

HARRY W. SHENTON III
MICHAEL J. CHAJES
J. HUANG

Department of Civil and Environmental Engineering
University of Delaware

Department of Civil Engineering
Widener University

November 2007

Delaware Center for Transportation
University of Delaware
355 DuPont Hall
Newark, Delaware 19716
(302) 831-1446

Load Rating of Bridges Without Plans

By

Harry W. Shenton, III
Michael J. Chajes
J. Huang

Department of Civil and Environmental Engineering
College of Engineering
University of Delaware

DELAWARE CENTER FOR TRANSPORTATION
University of Delaware
Newark, Delaware 19716

This work was sponsored by the Delaware Center for Transportation and was prepared in cooperation with the Delaware Department of Transportation. The contents of this report reflect the views of the authors who are responsible for the facts and accuracy of the data presented herein. The contents do not necessarily reflect the official views of the Delaware Center for Transportation or the Delaware Department of Transportation at the time of publication. This report does not constitute a standard, specification, or regulation.

The Delaware Center for Transportation is a university-wide multi-disciplinary research unit reporting to the Chair of the Department of Civil and Environmental Engineering, and is co-sponsored by the University of Delaware and the Delaware Department of Transportation.

DCT Staff

Ardeshir Faghri
Director

Jerome Lewis
Associate Director

Ellen M. Pletz
Assistant to the Director

Lawrence H. Klepner
T^2 Program Coordinator

Matheu J. Carter
T^2 Engineer

Sandra Wolfe
Secretary

DCT Policy Council

Robert Taylor, Co-Chair
Chief Engineer, Delaware Department of Transportation

Michael Chajes, Co-Chair
Dean, College of Engineering

The Honorable Tony DeLuca
Chair, Delaware Senate Transportation Committee

The Honorable Richard Cathcart
Chair, Delaware House of Representatives Transportation Committee

Timothy K. Barnekov
Dean, College of Human Resources, Education and Public Policy

Harry Shenton
Chair, Civil and Environmental Engineering

Ralph A. Reeb
Director of Planning, Delaware Department of Transportation

Stephen Kingsberry
Director, Delaware Transit Corporation

Shannon Marchman
Representative of the Director of the Delaware Development Office

Roger Roy
Representative, Transportation Management Association

Jim Johnson
Executive Director, Delaware River & Bay Authority

Delaware Center for Transportation
University of Delaware
Newark, DE 19716
(302) 831-1446

Load Rating of Bridges Without Plans

by H.W. Shenton III, M.J. Chajes, and J. Huang

DEPARTMENT OF
CIVIL & ENVIRONMENTAL ENGINEERING
UNIVERSITY OF DELAWARE

The Center For
INNOVATIVE
BRIDGE ENGINEERING

November 2007

Executive Summary

Most bridges in the United States are evaluated using simplified models that rely on structural dimensions and properties determined from original design plans and observations made during on-site inspection. However, it is common to have bridges for which structural plans do not exist or for which only partial plans exist. Many of these bridges without plans were built years ago.

Thompson [1999] conducted a survey and collected important data about bridges without plans in Delaware in Phase I of this project. In his survey, the 1997 Delaware Bridge Inventory was used to determine how many bridges in the state of Delaware have no original design plans and to identify the design type, date of construction, and materials of construction of these bridges. The search uncovered 189 bridges that have no original design plans. Of these, concrete (46%) and steel (37%) were the most common materials of construction. The most common design types were slabs, culverts, arch-decks, and stringer/multi-beams [Thompson, 1999]. In addition, many of Delaware's planless bridges have unknown dates of construction.

Bridges without plans pose a particular challenge to engineers and owners when these bridges have to be rated. Structural properties for bridges without original design plans are not easily obtained. This is especially a problem for older concrete bridges for which the amount of reinforcing steel may be unknown. As a result, the bridge capacity or rating cannot be evaluated easily using traditional methods, based on only simplified theoretical models.

Engineering judgment can be used, along with historical records and plans of similarly constructed bridges to arrive at plausible reinforcing details; however, these estimates tend to be conservative. As a result, load ratings for these bridges also tend to be very conservative, leading to load postings and traffic restrictions. Unnecessary load postings create much inconvenience for bridge users and a significant financial cost to the government. To avoid unnecessary load posting, the load-carrying capacity of a posted bridge should be determined accurately.

Load testing has been used extensively to assess bridge performance and capacity. Combining theoretical analysis and field tests can greatly enhance understanding of bridge performance for engineers. This idea can also be applied to evaluate the load-carrying capacity of bridges without plans. In Phase I of this project researchers at the University of Delaware developed two methodologies, the steel area method (SAM) and the simplified method (SM) to rate concrete bridges without plans using basic mechanics and beam theory and the results of a diagnostic load test [Thompson, 1999].

Phase 2 of the effort, initiated in 2003, was aimed at systematically validating the techniques for load rating bridges without plans developed in the earlier project and making recommendations on procedures to enable application of the techniques on a routine basis. A Ph.D. student affiliated with the UD Bridge Center carried out this work as part of his doctoral research. The following provides highlights of the findings of the research and testing.

Load rating bridges without plans is a difficult problem that bridge engineers and owners have to face, especially for concrete bridges without plans. The Steel area method (SAM) and the simplified method (SM), which incorporate the results of a diagnostic load test, have been developed to solve this problem. In this work, SAM was extended and then verified through

laboratory tests. A procedure for load rating bridges without plans based on SAM was proposed. The procedure was verified using a field test of a concrete slab bridge (Bridge 2-063), for which plans are available. In addition, load rating of bridges without plans using the simplified method (SM) was also illustrated. The following conclusions can be drawn from the study:

1. Equations for SAM have been extended to more general loading cases, i.e., that are representative of the multi-axle vehicles used in a diagnostic load test. By measuring the "moment-strain stiffness" or the "moment-deflection stiffness," the neutral axis location can be estimated and, subsequent to that, the area of reinforcing steel.

2. Laboratory tests on four beams (Standard, MMFX4, MMFX2, and CFRP beam) have been used to verify SAM. Based on the laboratory test results, the following observations can be made:

- The displacements measured in the test are more reliable than the concrete strains measured on the bottom of the beam. This is because the strains are affected by local cracking in the region of the strain gage.

- The cracking moments estimated based on theory are higher than the actual cracking moments measured in the tests, by about 30%. This has an effect on the area of steel estimated using the SAM.

- Provided the measured strain or deflection data is of sufficient quality, the SAM can provide a reasonable estimate of the area of reinforcing steel in the beam.

3. A procedure for load rating bridges without plans using SAM was proposed and verified using the field test of concrete slab Bridge 2-063. Based on the results of this investigation, the following conclusions can be drwan:

- The estimated steel areas are very reasonable. The average area estimated based on the concrete strains measured using BDI transducers with 12" extensions is less than the actual steel area by 31%. The average area estimated based on the displacement data is larger than the actual area by 38%. The errors can be attributed to the assumptions in the model and measurement error.

- The displacements measured using LVDTs and the strain data measured using BDI transducers with 12" extensions were more reliable and consistent than the concrete strain data measured using BDI transducers without extensions. In future tests of concrete slabs, BDI transducers should be used only with extensions.

- The procedure developed is sensitive to the load distribution factor.

- Although the load-rating factors for bridge 2-063 under the various rating trucks, calculated based on the estimated steel area, were not identical to those based on the actual steel area, they were still reasonable. For example, the operating level rating factor for the HS20T vehicle, based on the actual steel area is 2.13; the rating factors based on

the average steel areas determined from the stain and deflection data, are 1.24 and 3.17, respectively. The load-rating procedure based on SAM can provide very valuable information about concrete bridges without plans for bridge engineers and owners.

4. Rating factors based on SM are improved, i.e., higher than the theoretical rating factors. The improvement can be attributed to the fact that the in-situ information is included through SM. However, care must be taken in using SM when the diagnostic load test results are used to extrapolate the bridge response to higher load levels than used in the test. Where possible, both the SAM and SM methods should be used to arrive at a new load rating for the bridge.

Table of Contents

1. Introduction

Most bridges in the United States are evaluated using simplified models that rely on structural dimensions and properties determined from original design plans and observations made during on-site inspection. However, it is common to have bridges for which structural plans do not exist, or for which only partial plans exist. Many of these bridges without plans were built years ago.

Thompson conducted a survey and collected important data about the bridges without plans in Delaware [Thompson, 1999]. In his survey, the 1997 Delaware Bridge Inventory was used to determine how many bridges in the state of Delaware have no original design plans, and to identify the design type, date of construction and materials of construction of these bridges. The search uncovered 189 bridges that have no original design plans. Of these, concrete (46%) and steel (37%) were the most common materials of construction. The most common design types were slabs, culverts, arch-decks and stringer/multi-beams [Thompson, 1999]. In addition, many of Delaware's planless bridges have unknown dates of construction.

Bridges without plans pose a particular challenge to engineers and owners when these bridges have to be rated. Structural properties for bridges without original design plans are not easily obtained. This is especially a problem for older concrete bridges for which the amount of reinforcing steel may be unknown. As a result, the bridge capacity or rating cannot be evaluated easily using traditional methods, based on only simplified theoretical models.

Engineering judgment can be used, along with historical records and plans of similarly constructed bridges, to arrive at plausible reinforcing details; however, these estimates tend to be conservative. As a result, load ratings for these bridges also tend to be very conservative. Consequently, this can lead to unnecessary load postings and traffic restrictions for the bridges whose plans do not exist. Unnecessary load postings create much inconvenience for the bridge users and a significant financial cost to the government. In order to avoid unnecessary load posting, the load carrying capacity of a posted bridge should be determined accurately.

Load testing has been extensively used to assess bridge performance and capacity. Combining theoretical analysis and field tests can greatly enhance the understanding of the performance of the bridges for engineers. This idea can also be applied to evaluate the load carrying capacity of bridges without plans. Researchers at the University of Delaware developed two methodologies, the steel area method (SAM) and simplified method (SM), to rate concrete bridges without plans, using basic mechanics and beam theory, and the results of a diagnostic load test [Thompson, 1999].

In this report, first, the previous work on the SAM and SM are introduced briefly. Then SAM is extended and improved and equations are derived to accommodate more general load configurations. Laboratory tests are done to validate SAM. After that, a procedure for load rating bridges without plans incorporating the diagnostic load tests is proposed on the basis of SAM. A

concrete slab bridge with original structural drawings is chosen to validate the proposed procedures. In addition, the load rating for the bridge based on SM is illustrated.

2. Previous Work on Load Rating of Bridges without Plans at the University of Delaware

SAM and SM were developed by Thompson [Thompson, 1999]. In this section, the previous research done by Thompson is reviewed.

SAM uses strain or displacement measurements from field testing in conjunction with basic mechanics principles to estimate the unknown area of reinforcing steel in a concrete bridge. The estimated reinforcing steel area can then be used with traditional rating techniques. SM uses strain measurements from field testing combined with known material properties to directly estimate the load carrying capacity of a planless bridge [Thompson, 1999].

The two methods assume that the bridge works in the allowable stress limit during the test. Furthermore, the methods assume that the concrete slab can be modeled as a beam in the analysis. In addition, the following assumptions were adopted in the development of both methods:

- Plane sections remain plane (i.e., shear deformations are ignored)
- No slip between the reinforcing steel and the concrete
- Linear elastic materials

2.1 Steel Area Method

2.1.1 Theoretical Derivation

Consider a simply supported (SS) rectangular beam with a span of L which is loaded at midspan with a concentrated force P. The dimensions of the beam and the assumed strain and stress distribution are shown in Figure 2.1.

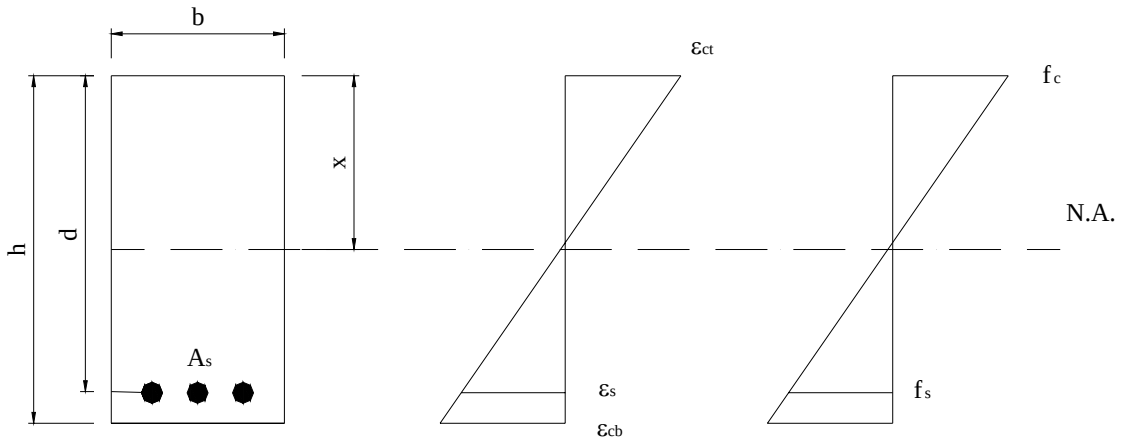

(a) Cross section of concret beam (b) Strains (c) Stresses

Figure 2.1 Assumed Strain and Stress Distribution

The variables needed to derive equations are defined below:
d = the distance between the top of the beam and the reinforcing steel
b = the beam width
h = the beam depth
x = the distance from the top fiber of the beam to the neutral axis
L = the span length
E_c = the Young's modulus of concrete
E_s = the Young's modulus of the reinforcing rebar
A_s = the area of reinforcing rebar
n = E_s/E_c
f_s = stress in rebar
f_c = the compressive stress of concrete on the top fiber of the beam
ε_{ct} = the strain of concrete on the top fiber
ε_{cb} = the tensile strain of concrete on the bottom fiber
ε_s = the tensile strain of the rebar

In the derivation, the tensile concrete is assumed to be cracked. The internal compressive force within the concrete can be expressed as

$$C = 0.5 f_c bx = 0.5 E_c \varepsilon_{ct} bx \tag{1}$$

The resultant tensile force in the reinforcing steel is

$$T = f_s A_s = E_s \varepsilon_s A_s \tag{2}$$

Equating (1) to (2) gives

$$\frac{f_s}{f_c} = \frac{bx}{2A_s} \tag{3}$$

From the two assumptions that the linear strain relationship stands across the transverse section and that stress is proportional to strain, they yield

$$\frac{\varepsilon_s}{\varepsilon_{ct}} = \frac{d-x}{x} \tag{4}$$

$$\frac{f_s}{f_c} = \frac{E_s \varepsilon_s}{E_c \varepsilon_{ct}} = n\frac{d-x}{x} \tag{5}$$

The following equation for the neutral axis can be obtained by equating Equations 4 and 5:

$$\frac{bx^2}{2} = nA_s(d-x) \tag{6}$$

The steel rebar strain and the strain at the bottom fiber of the concrete beam can be related based on the linear strain relationship:

$$\varepsilon_s = \varepsilon_{cb}\left[\frac{d-x}{h-x}\right] \tag{7}$$

The internal moment is given by

$$M_n = A_s E_s \varepsilon_s (d - \frac{x}{3}) = A_s E_s \varepsilon_{cb}\left[\frac{d-x}{h-x}\right](d - \frac{x}{3}) \tag{8}$$

The moment for a SS beam loaded by a concentrated load P at midspan is given by

$$M_n = \frac{PL}{4} \tag{9}$$

Substituting (9) into Equation (8) yields

$$\frac{PL}{4} = A_s E_s \varepsilon_{cb}\left[\frac{d-x}{h-x}\right](d - \frac{x}{3}) \tag{10}$$

Rearranging (10) yields

$$k_{E_\varepsilon} = \frac{P}{\varepsilon_{cb}} = \frac{4A_s E_s\left[\frac{d-x}{h-x}\right](d - \frac{x}{3})}{L} \tag{11}$$

Equation (11) defines the slope of the concentrated load P versus concrete bottom strain and was referred to as the "strain stiffness." When the strain stiffness is obtained from the load vs. strain plot recorded in a test, equations (6) and (11) can be used to solve for the unknowns x and A_s.

Equations were also derived to determine the reinforcing steel area using displacement data for the SS beam loaded by a concentrated load P at midspan. Assume that the deflection of the beam at midspan is measured and the section is cracked under its own weight. The moment of inertia for the cracked section is

$$I_{cr} = \frac{1}{3}bx^3 + nA_s(d-x)^2 \tag{12}$$

Therefore, the deflection at midspan is given by

$$\delta = \frac{PL^3}{48E_cI_{cr}} \tag{13}$$

Rearranging Equation (13) yields

$$k_{E_\delta} = \frac{P}{\delta} = \frac{48E_cI_{cr}}{L^3} \tag{14}$$

Equation (14) defines the slope of the load vs. displacement and was referred as the "displacement stiffness" of the beam. If the displacement stiffness is obtained from a test, Equations (6) and (14) can be used to determine the unknowns x and A_s.

2.1.2 Experimental Verification

Experimental verification, including laboratory tests and a diagnostic test, were done to verify the SAM and SM.

Laboratory Test

A limited experimental investigation was conducted in the laboratory using three under–reinforced rectangular beams in order to test SAM at the University of Delaware [Thompson 1999]. The specimens tested measured 4 inches by 5 inches and were 46 inches in length. The beams were fabricated with different amounts of reinforcing steel: one beam with a single #3 rebar, one beam with a single #4 rebar, and one beam with a single #5 rebar. Displacement and strains due to a three point bending tests were measured for each test. The beam was first tested in its pre-cracked state by loading to 80% of its ultimate strength, and then tested in its cracked state by loading up to failure.

Although the area of steel predicted using the measured strain and deflection data was of the correct order of magnitude, the trends for moment-strain stiffness and moment-deflection stiffness were not consistent with the theoretical analysis. Some factors that may have contributed to the poor experimental results are (1) difficulty in accurately measuring low stains and displacements of small-scale concrete beams, (2) improperly bonded strain transducers and (3) placement or location of the reinforcing steel in the specimens [Thompson 1999]. It is also found that SAM based on the strain stiffness is relatively insensitive to experimental error.

Field Test

The University of Delaware performed diagnostic load tests on five bridges along U.S. Route 13 in November of 1998. These tests were part of a University of Delaware project funded by Delaware Department of Transportation (DelDOT). While the primary purpose of the load testing was to evaluate permit vehicle capacity for these bridges, the data was also used here to test the methods developed for evaluating planless bridges. Bridge 1-450 was chosen to illustrate and verify SAM and SM because it had the highest recorded strains of the five bridges tested [Thompson 1999].

Northbound Bridge 1-450 was built in 1931. This bridge has a span of $8\ ft$, a $10\ in$ section depth and $3\ ksi$ concrete design strength. Two feet of material (i.e., fill or overburden), which consists of a combination of an old concrete roadway and soil, exists between the asphalt-wearing surface and the superstructure.

Twelve Bridge Diagnostics Inc. (BDI) strain transducers were installed on the bottom surface of the concrete slab, nine strain transducers measuring three inches in length and three strain transducers measuring 12 inches. The three-inch transducers are sufficient to monitor compressive strains in concrete; however, they may not provide accurate strain readings for concrete in tension when cracking occurs. Twelve-inch transducers allow an average strain to be taken over a longer gage length and minimize the effect of high-localized strains resulting from tensile cracking. The test vehicle was a three-axle, truck with a total weight of 29.6 tons. Reference markers were made in the roadway to locate the truck paths relative to the gages. The first load test was conducted using ambient traffic conditions. The second load test was conducted with the driver wheel line moving forward and backward along the white chalk line, which was used to determine the load path directions. The third load test was conducted with the passenger wheel line moving forward and backward along the white chalk line.

The results showed that when the effect of the superstructure, fill and concrete roadway are included, the estimated steel area was relatively close to the actual reinforcing steel area. In addition, the conclusion that the distribution factor plays an important role in SAM can be drawn.

2.1.3 Discussion

Thompson's theoretical derivation was based on the simplest model, which is a SS beam loaded by a single concentrated load at midspan. This may be suitable for a bridge with a span length much greater than the test vehicle axle spacing; however, for shorter span bridges, modeling the test truck as a single concentrated load is a crude approximation that can lead to errors in the estimated area of steel. In Section ?.?, SAM is theoretically extended and improved to accommodate more complicated load cases.

Although laboratory tests and a field test were done to verify SAM, some limitations about these tests exist. For the laboratory test, the poor experimental results can be attributed to the small-scale beam and poor test set-up. It is difficult to accurately measure the strain and deflection for this small beam under small loads.

For the field test, Bridge 1-450, which is a box culvert, was tested as part of another project and was not selected for the primary purpose of validating the two methods. This culvert was not the ideal structure to use to evaluate SAM because of its very short span and the presence of almost two feet of fill and roadway on top of the superstructure. While the results were encouraging, the test cases did not lend themselves to a systematic evaluation of SAM.

In order to systematically validate SAM and recommend a procedure for load rating a bridge without plans, more tests in the laboratory and a suitable field test should be conducted to verify the method. In the later part of this chapter, laboratory tests results on large-scale beams are used to verify SAM. Then, the procedure for load rating bridges without plans is proposed. Finally, a concrete slab bridge in good condition, which is an ideal structure to test SAM, was tested and the results used to evaluate SAM and validate the proposed procedure.

2.2 Simplified Method

The simplified method (SM) developed previously uses strain measurements from the field test combined with known material properties to directly estimate the bridge load rating. The rating is based on observed live load strain as compared to total allowable strain values.

In terms of strain, for load rating according to allowable stress, the rating equation can be expressed as

$$RF = \frac{\varepsilon_{all} - \varepsilon_{DL}}{\varepsilon_{LL}(1+I)} \tag{15}$$

where RF = rating factor; ε_{all} = allowable strain; ε_{DL} = dead load strain; ε_{LL} = live load strain; and I = impact factor.

For concrete bridges designed by the allowable stress method, the maximum allowable service load strain ε_{LL} for the rebars in the inventory load rating level is taken to be

$$\varepsilon_{all} = \frac{0.55 f_y}{E_s} \tag{16}$$

This can be estimated with reasonable confidence from the age of the bridge and with knowledge of the grade of reinforcing steel common for that era.

The live load strains ε_{LL} under rating truck level can be estimated based on the measured maximum strain in the diagnostic test. Suppose that both the dead load moment and the moment due to the test truck act on the cracked section, the dead load strains can also be obtained by the simple relationship,

$$\varepsilon_{DL} = \left(\frac{M_{DL}}{M_{LL}}\right)\varepsilon_{LL} \tag{17}$$

where, M_{DL} and M_{LL} are the theoretical moments due to dead load and live load produced by the test truck, respectively; ε_{LL} is the measured maximum strain under the test truck.

The advantage of SM is that no estimation of the reinforcing steel area is needed. However, this method is only an approximate technique and provides bridge engineer a simple way for determining valuable information that can be used to re-evaluate low posting level.

3. Development of Steel Area Method for General Load Cases

3.1 Estimating Steel Area Using Strain Data

Consider a SS rectangular beam with span length *L*. The geometry of the beam, and the assumed stress and strain distributions are shown in Figure 2.1.

Force equilibrium in the cross section of the beam requires that the resultant tensile force in the rebar is equal to the resultant compressive force in the concrete, i.e.,

$$E_s \varepsilon_s A_s = \frac{E_c \varepsilon_{ct} bx}{2} \tag{1}$$

Strain compatibility also requires

$$\frac{\varepsilon_s}{\varepsilon_{ct}} = \frac{d-x}{x} \tag{19}$$

Solving equations (1) and (19) for the area of steel yields

$$A_s = \frac{bx^2}{2n(d-x)} \tag{20}$$

Appling strain compatibility between the rebar and the bottom concrete yields

$$\frac{\varepsilon_{cb}}{\varepsilon_s} = \frac{h-x}{d-x} \tag{21}$$

The resultant moment on the cross section is given by

$$M = A_s E_s \varepsilon_s (d - \frac{x}{3}) \tag{22}$$

Moving ε_s to the left-hand side of Equation (22) and substituting Equation (20) yields

$$\frac{M}{\varepsilon_s} = A_s E_s (d - \frac{x}{3}) = E_c \frac{bx^2 (d - \frac{x}{3})}{2(d-x)} = k_{strain} \tag{23}$$

Substituting Equation (21) into Equation (23) yields

$$\frac{M}{\varepsilon_{cb}} = E_c \frac{bx^2 (d - \frac{x}{3})}{2(h-x)} = k_{strain} \tag{24}$$

Equation (23) or Equation (24) is the expression for what will be referred to as the "moment-strain stiffness," i.e., the ratio of the applied moment to the strain of rebar or bottom concrete. It is similar to equation (11) derived by Thompson, with the exception that it is expressed in terms of the internal moment *M*, modulus of the concrete, and the area of steel has been eliminated from the equation. It is more versatile than the equation derived by Thompson, since it is expressed in terms of a general moment *M*, which can be due to a single concentrated load, or a combination of loads, like that produced by a multi-axle test truck. The equation is a function of the modulus of the concrete, depth and width of the section, depth to the tension rebar and the neutral axis depth. By measuring the moment-strain stiffness, and assuming or measuring E_c, b and d, the depth to the neutral axis x can be calculated from the cubic algebraic equation, which could be solved by commercial software, such as MATLAB and MAPLE. Once the neutral axis is determined, knowing the modulus of the steel, the area of reinforcing rebar can be estimated using Equation (20).

3.2 Estimating Steel Area Using Deflection Data

Assume that deflections caused by a loaded vehicle or any other loads are measured at midspan of a SS beam with constant section. The deflection at midspan (Δ) calculated by the principle of virtual work can be expressed as

$$\Delta = \int_0^L \frac{\overline{M}_K M_p}{E_c I_e} ds = \frac{M_{correct}}{E_c I_e} \tag{25}$$

where,

$$M_{correct} = \int_0^L \overline{M}_K M_P ds \tag{26}$$

$\overline{M}_K$ is the bending moment in the beam due to a unit virtual force at midspan, and M_P is the bending moment in the beam caused by the loaded truck of known weight and axle spacing or any other loads, in a certain location on the beam. I_e in equation (25) is the effective moment of inertia of the section, which is given by [AASHTO LRFD, 1998]

$$I_e = \left(\frac{M_{cr}}{M_a}\right)^3 I_g + \left[1 - \left(\frac{M_{cr}}{M_a}\right)^3\right] I_{cr} \le I_g \tag{27}$$

in which

$$M_{cr} = f_r \frac{I_g}{y_t} \tag{28}$$

where M_{cr} is the cracking moment of the section, f_r is the modulus of rupture of concrete, and y_t is the distance from the neutral axis to the extreme tension fiber. In Equation (27), M_a is the maximum moment in a component at the stage for which deformation is computed, I_g is the moment of inertia of the gross uncracked section, and I_{cr} is the moment of inertia of the cracked section, which for a rectangular section of width b is given by

$$I_{cr} = \frac{1}{3} b x^3 + n A_s (d - x)^2 \tag{29}$$

Solving equation (25) for E_cI_e and substituting equation (27) into it yields, in the case of $I_e \le I_g$,

$$\frac{M_{correct}}{\Delta} = E_c I_e = E_c \left\{ \left(\frac{M_{cr}}{M_a} \right)^3 I_g + \left[1 - \left(\frac{M_{cr}}{M_a} \right)^3 \right] I_{cr} \right\} \tag{30}$$

Now substituting M_{cr} from equation (28), I_{cr} from equation (29) and A_s from equation (20) into equation (30) yields

$$\frac{M_{correct}}{\Delta} = E_c \left\{ \left(\frac{f_r \frac{I_g}{y_t}}{M_a} \right)^3 I_g + \left[1 - \left(\frac{f_r \frac{I_g}{y_t}}{M_a} \right)^3 \right] \left[\frac{1}{3} b x^3 + \frac{b x^2 (d - x)}{2} \right] \right\} = k_{defl} \tag{31}$$

Equation (31) is the expression for what will be referred to as the "moment-deflection stiffness;" i.e., the ratio of the applied moment to the deflection at midspan of the beam. Once again, this expression of the SAM is more versatile than the one derived by Thompson, as it is expressed in terms of a generalized moment (Equation 26), that can be due to a single concentrated load, or a combination of loads, like that produced by a multi-axle truck. It is effectively equal to the flexural stiffness of the section, and is a function of the modulus of the concrete, depth and width of the section, depth to the tension reinforcement, the neutral axis depth, modulus of rupture of concrete, gross moment of inertia and the maximum moment M_a. By measuring the moment-deflection stiffness, assuming or measuring E_c and f_r, and assuming or measuring b, d and y_t, the depth to the neutral axis x can be calculated from the cubic algebraic equation, which could be solved by commercial software such as MATLAB or MAPLE. Once the neutral axis is determined, knowing the modulus of the rebar, the area of reinforcing steel can be estimated by equation (20).

For FRP reinforced beams, Equation (27) can overestimate the effective moment of inertia because the bond characteristics of FRP bars affect the deflection of a member [ACI 440.1R-01]. To account for the lower modulus of elasticity and the bond behavior of FRP reinforcement, a modified expression for the effective moment of inertia is recommended and is given by [ACI 440.1R-01]:

$$I_e = \left(\frac{M_{cr}}{M_a} \right)^3 \beta_d I_g + \left[1 - \left(\frac{M_{cr}}{M_a} \right)^3 \right] I_{cr} \le I_g \tag{32}$$

$$\beta_d = \alpha_b \left[\frac{E_f}{E_s} + 1 \right] \tag{33}$$

where E_f is the modulus of elasticity of FRP reinforcement, and the recommended value for α_b is 0.5 for all FRP bar types.

Therefore, the counterpart of equation (31) for a beam reinforced with FRP rebar is, in the case of $I_e \le I_g$,

$$\frac{M_{correct}}{\Delta} = E_c \left\{ \left(\frac{f_r \frac{I_g}{y_t}}{M_a} \right)^3 \beta_d I_g + \left[1 - \left(\frac{f_r \frac{I_g}{y_t}}{M_a} \right)^3 \right] \left[\frac{1}{3} b x^3 + \frac{b x^2 (d - x)}{2} \right] \right\} = k_{defl} \qquad (34)$$

The theoretical prediction for deflection depends greatly on the cracking moment of the beam, which is usually estimated using Equation (28). Laboratory tests conducted by Ashour showed that using f_r to compute the cracking moment overestimates the value, and this overestimation increases as the concrete compressive strength increases [Ashour, 2000]. Ashour pointed out that the cracking moment obtained using f_r overestimates the actual cracking moment by 1.5-2.0 times.

A similar conclusion can be drawn from the laboratory test done by McNally at the University of Delaware [McNally, 2003]. McNally tested four reinforced concrete beams. One beam (referred to as “Standard” beam) was reinforced with standard steel rebar; two others were reinforced with MMFX rebar (referred to as “MMFX4” and “MMFX2” beam, respectively); and one other beam was reinforced with Carbon Fiber Reinforced Polymer (CFRP) rebar (referred to as “CFRP” beam).

Table 3.1 Theoretical and Measured Cracking Moments for Four Different Reinforced Concrete Beams (Unit: ft-lb) (McNally, 2003)

	Standard beam	MMFX4 beam	MMFX2 beam	CFRP beam
Theoretical (Eq. ((28))	63,520	67,010	67,010	62,410
Measured	48,385	44,230	42,818	41,196
Theoretical/Measured	1.31	1.52	1.56	1.51

Table 3.1 presents the theoretical value and test results for cracking moment of the four beams. The ratio of the theoretical value to the measured cracking moment of the standard beam is around 1.3, and for the other three beams is around 1.5. These results suggest that the cracking moment M_{cr} predicted by Equation (28) needs to be reduced by a factor of 1.3-1.5 when used in SAM.

3.3 Laboratory Verification of the Modified Steel Area Method

A test program was conducted to study the use of MMFX and CFRP rebar in the reconstruction of Bridge 1-712B, which is located in the Interstate-95 service area in Newark, Delaware [McNally 2003]. The program included four 20' long concrete beams that were reinforced with MMFX, CFRP and standard grade 60 rebar. The cross section of the test beams were 16 inches wide by 20 inches deep. Each beam was tested to failure in four point bending. Though the test program was part of another project, the data collected from these four beams can be used to verify the SAM herein.

3.3.1 Design of the Test Beams

The first beam was designed with 4-#6 standard grade 60 rebar in the tension zone. This Standard beam acts as a reference for the other test beams. The second beam (referred to as "MMFX4") was designed with MMFX rebar and had the same amount of MMFX flexural reinforcement as the standard grade 60 beam. The third beam (referred to as "MMFX2") was designed with MMFX rebar but had half the reinforcement of the standard Grade 60 and the other MMFX beam. The final beam (referred to as "CFRP") was designed with 4-#6 CFRP rebar in the tension zone. The design of the last beam was not controlled by strength, as was the case for the Standard beam and the MMFX beams; the CFRP beam design was deflection controlled. Though the CFRP beam was stronger in flexure than necessary, it just satisfied the deflection criteria [McNally, 2003].

All four beams have the same dimensions and geometry, that is, 16 inch width, 20 inch depth and 20 feet span length. The rebars for each beam are located a distance "*d*" of 17.5 inches down from the top of the beam. The concrete strength used in the design of the four beams was 12 *ksi*. The shear reinforcement in all the beams consisted of #4 grade 60 stirrups, spaced evenly throughout the beam at 8 inches on center for the Standard, MMFX4 and MMFX2 beams, and spaced evenly at 4 inches for the CFRP beam. The shear capacity for all the test beams was designed to eliminate shear as a failure mode.

Cross section and elevation views of the Standard, MMFX4, MMFX2, and CFRP beams are shown in Figures 3.1 through 3.4, respectively.

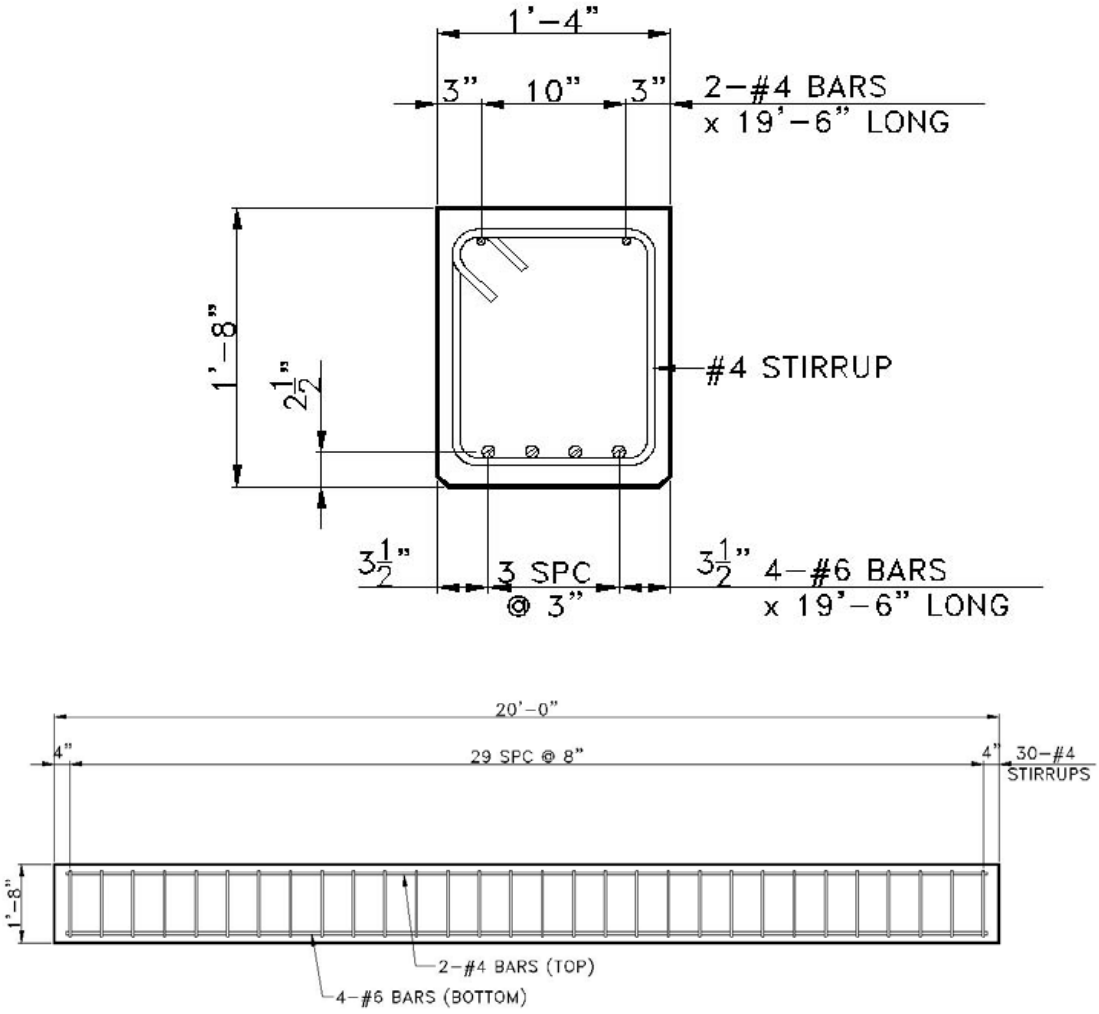

Figure 3.1 Cross Section and Elevation of Standard Beam [McNally, 2003]

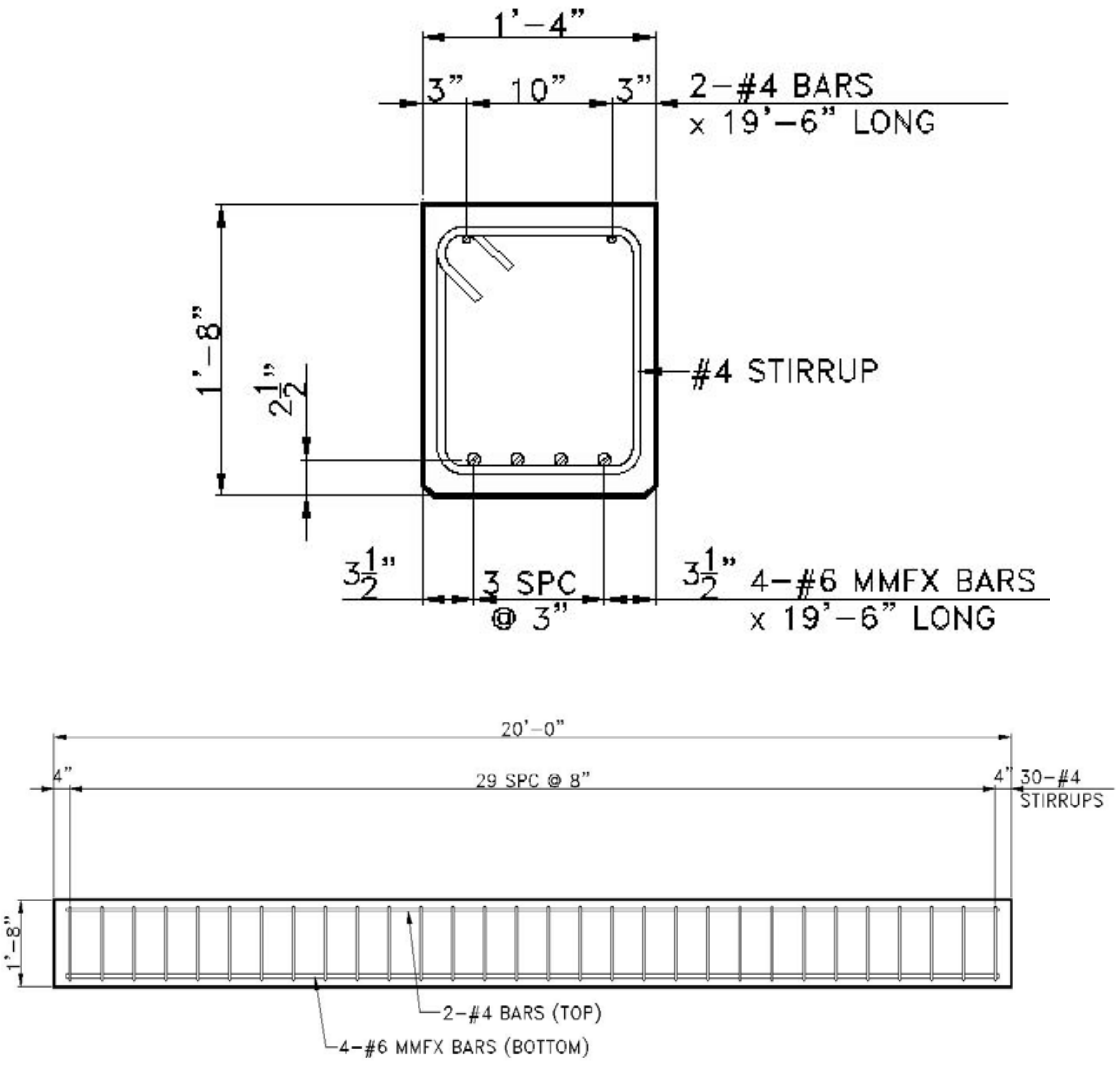

Figure 1.2 Cross Section and Elevation of MMFX4 Beam [McNally, 2003]

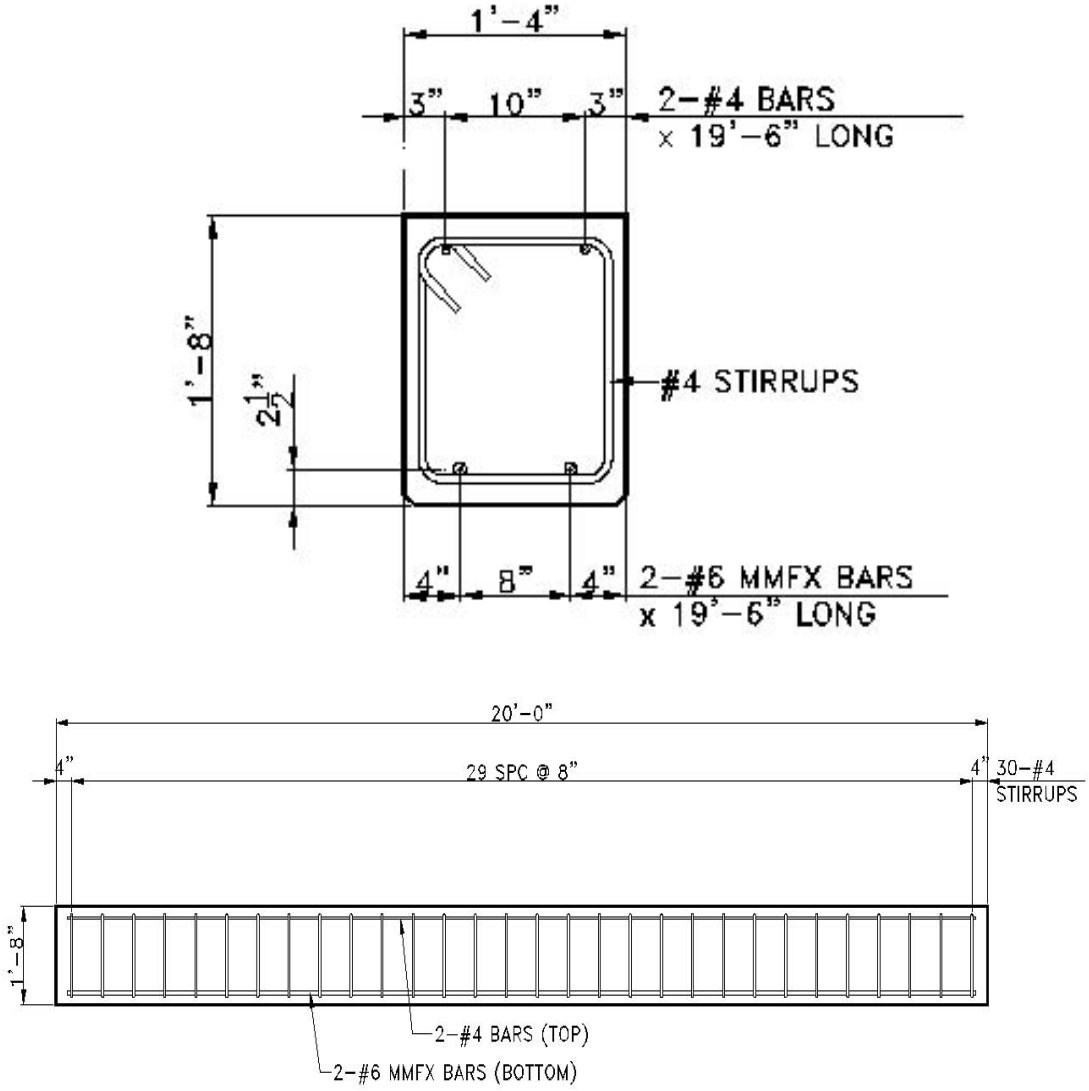

Figure 3.3 Cross Section and Elevation of MMFX2 Beam [McNally, 2003]

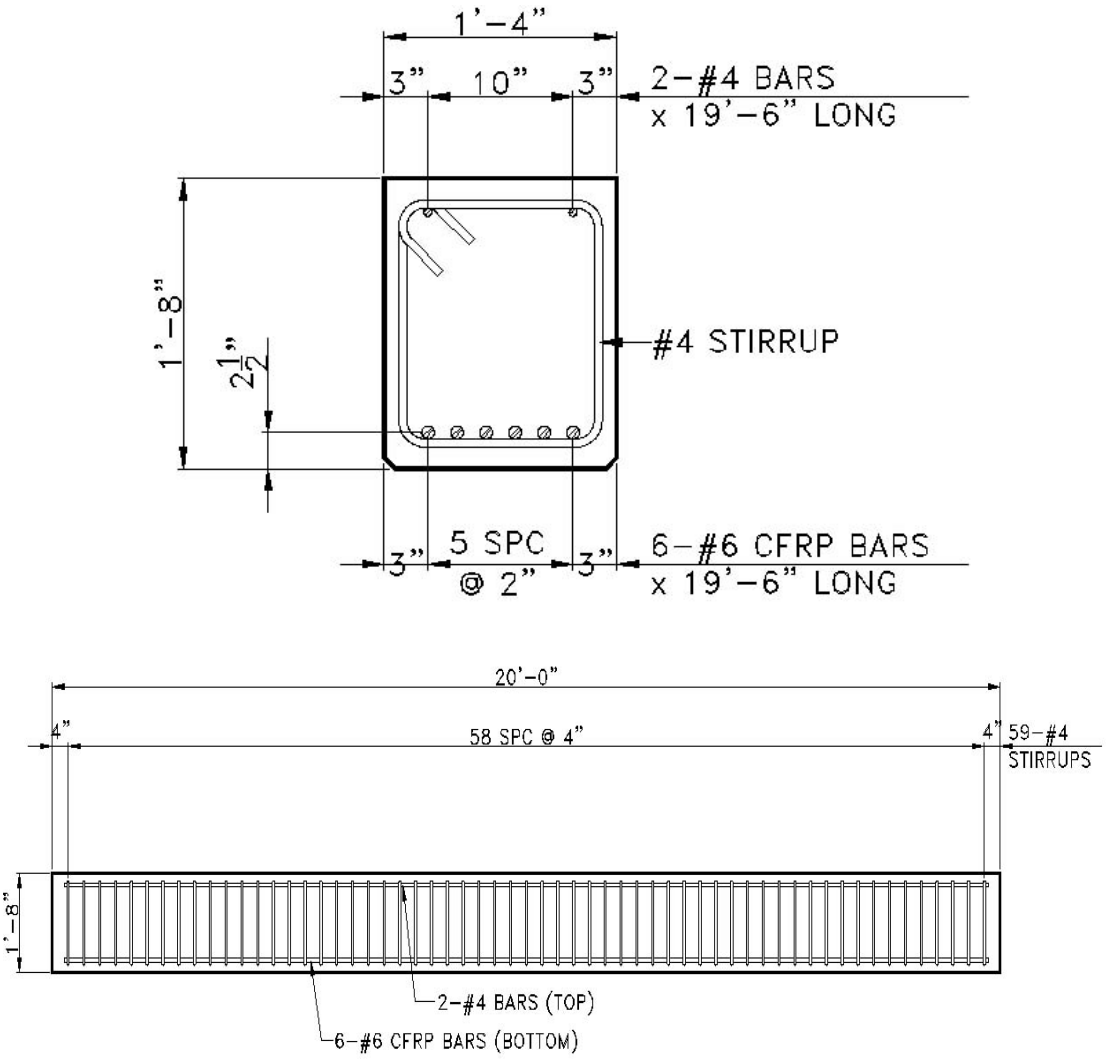

Figure 3.4 Cross Section and Elevation of CFRP Beam [McNally, 2003]

3.3.2 Material Properties

Table 3.2 presents the strength of the concrete obtained from cylinder tests. Three tensile tests were performed on the MMFX, standard grade 60, and the CFRP rebar. The properties of the rebar were calculated from the results of the tensile tests. Table 3.3 presents the properties of the materials (note that the researchers were not able to test the CFRP rebar to failure).

Table 3.2 Concrete Strength of Test Beams [McNally, 2003]

MMFX Beam Cylinders		Standard Beam Cylinders		CFRP Beam Cylinders	
Test #	Stress (psi)	Test #	Stress (psi)	Test #	Stress (psi)
1	10740.0	1	8796.0	1	8024.0
2	9286.0	2	8965.0	2	9630.0
3	10280.0	3	9472.0	3	8640.0
Avg = 10.10 ksi		Avg = 9.08 ksi		Avg = 8.76 ksi	

Table 3.3 Flexural Reinforcement Properties [McNally, 2003]

Material	Test #	Yield Point (ksi)	Ultimate (ksi)	Modulus (ksi)
MMFX #6 Bar	1	125.2	181.2	30,200
	2	127.3	181.0	30,300
	3	118.5	181.2	34,400
Average		123.7	181.1	31,633
Grade 60 #6 Bar	4	64.5	101.1	28,400
	5	64.1	101.2	35,400
	6	64.4	101.5	30,100
Average		64.3	101.3	31,300
CFRP #6 Bar	7	N/A	N/A	24,100
	8			23,400
	9			22,200
Average		N/A	N/A	23,233

3.3.3 Test Procedure

Two MTS 150 kip actuators, spaced 4 feet apart at the center of each beam, were used to create the constant moment region. Loading plates and rollers were placed between the actuator and beam to distribute the load evenly and to prevent local crushing of the concrete. Figure 3.5 shows the actuator locations in the tests.

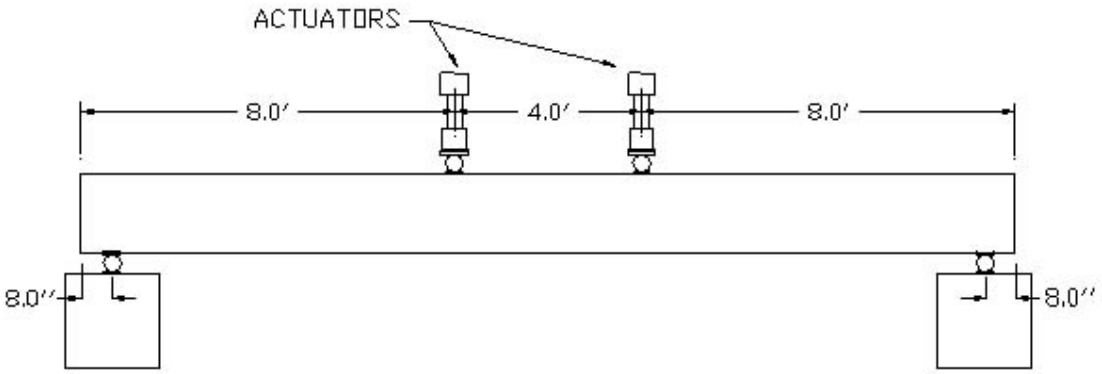

Figure 3.5 Actuators on Beams [McNally, 2003]

Resistive foil strain gages, mounted on 16-inch "sister" bars, which were embedded in the beams during fabrication, were used to measure the internal strain in both the tension and compression regions of each beam. The internal strain gages, located at the center of the beam, 2.5 inches up from the bottom and 2.625 inches down from the top surface of the beam, were read using a MicroMeasurements System 5000 data acquisition system [McNally, 2003]. Strain transducers (BDI) placed along the top and bottom of the beam were used to measure the strain on the external fibers of the beam. On the bottom of the beam, only three-inch BDIs were used to measure the concrete strains. On the top of the beam at the midspan, one three-inch, one six-inch and one twelve-inch BDI were used to measure the strain Figure 3.6 illustrates the locations of the sister bars and BDI gages.

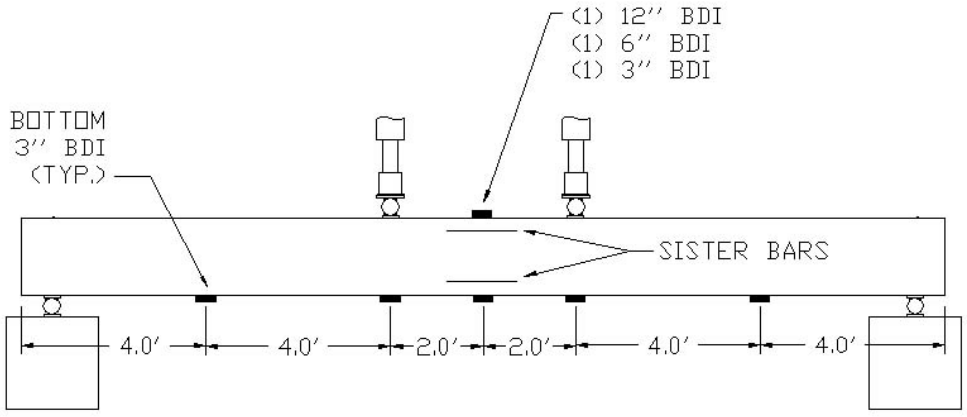

Figure 3.6 BDI and Sister Bar Locations [McNally, 2003]

Displacements were measured using LVDTs, which were placed beneath the beam and along its length. The locations of the LVDTs were at the center of the beam, at the two loading points, and at the end supports of the beam. Figure 3.7 shows the location of the LVDTs.

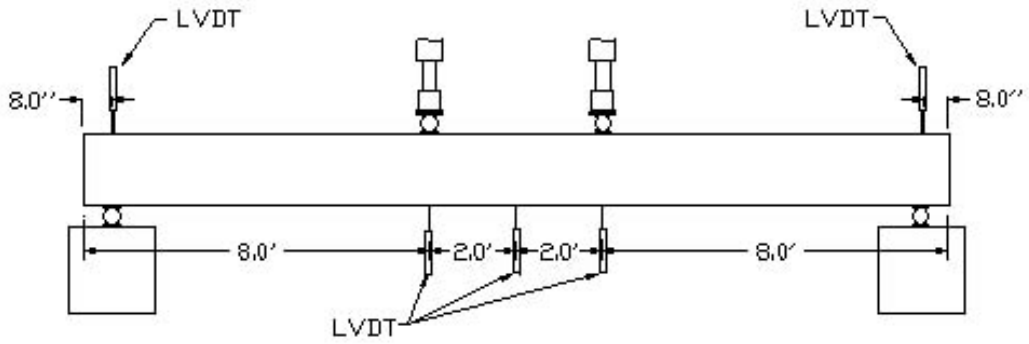

Figure 3.7 LVDT Location [McNally, 2003]

Figure 3.8 Typical Test Setup [McNally, 2003]

A typical test set-up is shown in Figure 3.83.8. Each beam was subjected to three load cycles. The first load cycle was done to just crack the beam. In order to accomplish this, for the Standard beam it was loaded up to 12 kips per actuator and then unloaded. For the two MMFX and CFRP beams, they were loaded up to 10 kips per actuator and then unloaded. The second load cycle repeated the first one. This second load cycle was used to make sure that the beam performed in a linear fashion after concrete cracking in the tensile region. The third load cycle involved loading the beam to failure. The BDI gages were removed in the third load cycle because of the high loads in this phase.

3.3.4 Analysis of Test Result

McNally analyzed the test data to validate the design methods and the performance of MMFX and CFRP rebar in his thesis [McNally 2003]. In this section, the analysis is focused on the validation of SAM. The test data from the second load cycle for each beam is selected in the following analysis.

Figures 3.9, 3.10, and 3.11 illustrate the histories of strain in the tensile sister bar, strain on the bottom of the beam, and the deflection at midspan of the Standard beam, respectively. From Figures 3.9 and 3.11, the linear relationship between the response and load is observed for the strain in the sister bar and deflection in the entire loading and unloading phases. For the other three beams, linearity is also observed for the strain in sister bar and the deflection at midspan.

From Figure 3.10, it is observed that in the loading phase, the linearity is shown under the load below around 6,000 lbs; after that, the microstrain does not change with the load increasing. The same phenomenon is observed in the tensile concrete microstrain data for MMFX2 beam. We can see, even if in the laboratory, accurately measuring microstrain for concrete in tensile area is not an easy job due to the local cracking of the concrete. For example, the measurement about the microstrain on bottom for CFRP beam failed in the test for the data recorded is negative. In addition, part of the recorded tensile concrete strain data for MMFX4 beam is missing. Therefore, the tensile concrete strain data for CFRP beam and MMFX4 beam are not going to be used.

The first step to estimate the rebar area is to determine the moment-strain stiffness defined in equation (23) or (24), or moment-deflection stiffness defined in equation (30) or (31). Linear regression is used to obtain the moment-strain stiffness and moment-deflection stiffness. In order to do the linear regression, the load and corresponding strain or deflection was chosen at around every one thousand pounds. The moment at midspan in equation (23) or (24) is calculated from the load based on the equilibrium equation. $M_{correct}$ at the midspan in equation (30) or (31) is calculated from the load based on equation (26). After that, the load vs. strain is converted to moment vs. strain and the load vs. deflection is converted to $M_{correct}$ vs. deflection. Finally, by the linear regression analysis, moment-strain stiffness defined in equation (23) or (24), or moment-deflection stiffness defined in equation (30) or (31) is obtained.

The linear regressions of moment-strain stiffness in terms of the tensile steel strain (the strain measured at the sister bar in the tensile area) and moment at midspan are shown in Figure 3.12, Figure 3.15, Figure 3.17 and Figure 3.19, for the four beams. The theoretical and measured values for moment-strain stiffness based on the tensile steel strain are presented in Table 3.4.

The linear regressions of moment-strain stiffness in terms of the bottom concrete strain and the moment at midspan are shown in Figures 3.13 and 3.20 for the Standard Beam and the MMFX2 Beam, respectively. For the MMFX4 Beam, the part of the recorded data for the

concrete strain on the bottom of beam was missing in the original data file, and for the CFRP Beam, all of the concrete strain on the bottom of the beam was negative. Therefore, these data were not used in the analysis. The theoretical and measured values for moment-strain stiffness based on the bottom concrete strain and moment are presented in Table 3.5.

The linear regression of moment-deflection stiffness is shown in Figure 3.14, 3.16, 3.18, and 3.21 for the Standard Beam, MMFX4 Beam, CFRP Beam, and MMFX2 Beam, respectively. The theoretical and measured values for moment-deflection stiffness are presented in Table 3.6.

After the moment-strain stiffness in terms of the tensile steel strain is known, Equations (23) and (20) are used to estimate the rebar area. Similarly, Equations (24) and (20) are used to estimate the rebar area when the values for the measured moment-strain stiffness in terms of the bottom concrete strain are available. Also, Equation (30), (31), or (34) with Equation (20) is used to estimate the rebar area if the measured moment-deflection stiffness is obtained. The measured cracking moment M_{cr} from Table 3.1 is used in the respective equations. The maximum moment M_a in Equation (30), (31) or (34) is calculated as the moment due to the maximum test load in the post-cracking phase plus the dead load moment at midspan. Table 3.7 shows the estimated rebar area by different moment-strain stiffness or moment-deflection stiffness for the four beams.

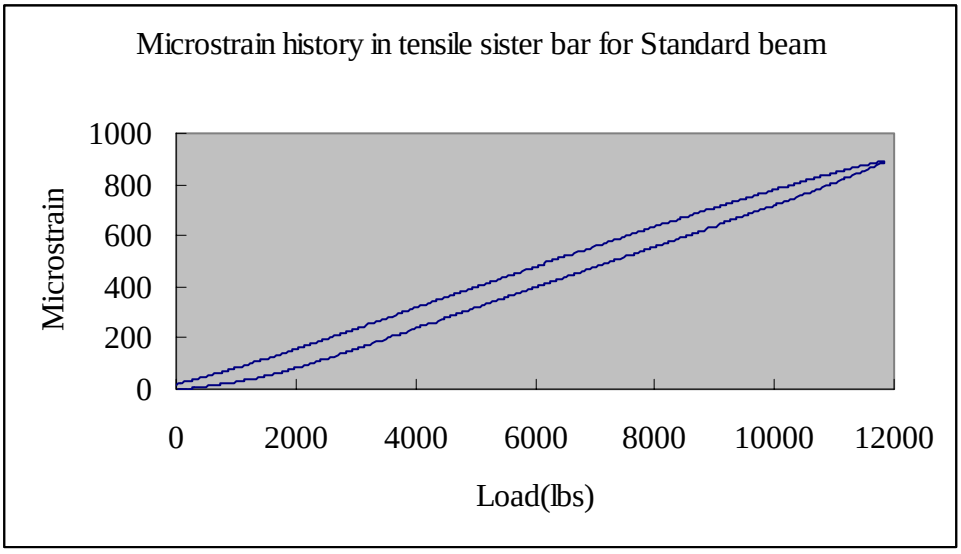

Figure 3.9 Microstrain History in Tensile Sister Bar for Standard Beam

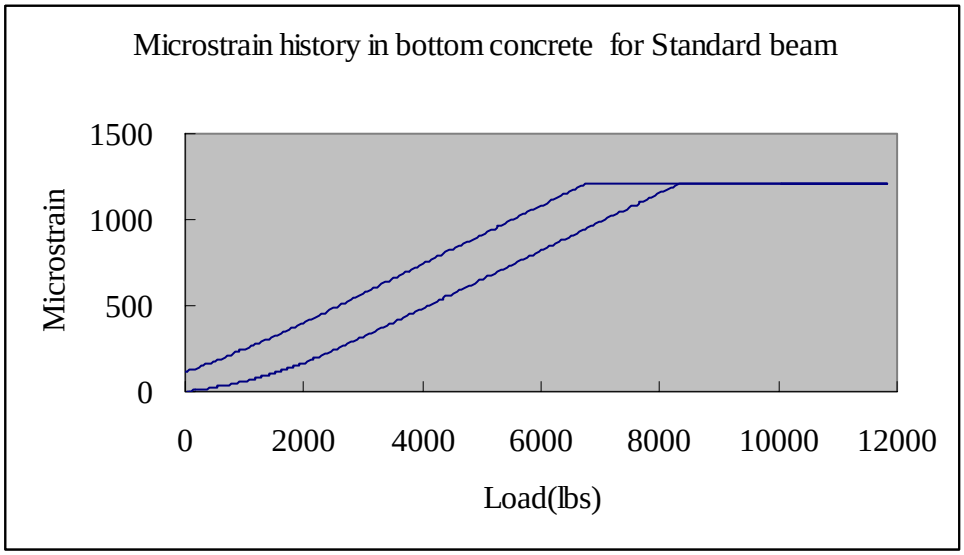

Figure 3.10 Microstrain History in Bottom Concrete at Midspan for Standard Beam

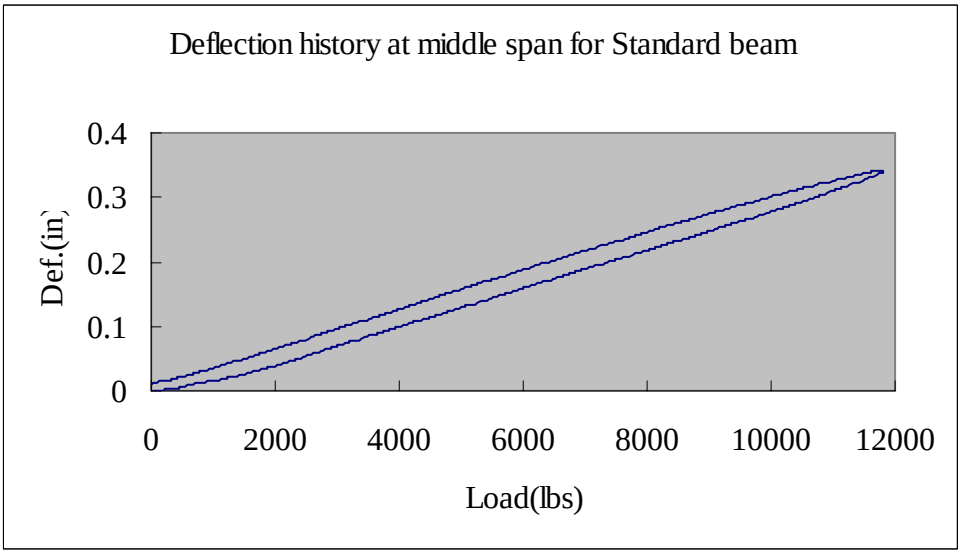

Figure 3.11 Deflection History at Midspan for Standard Beam

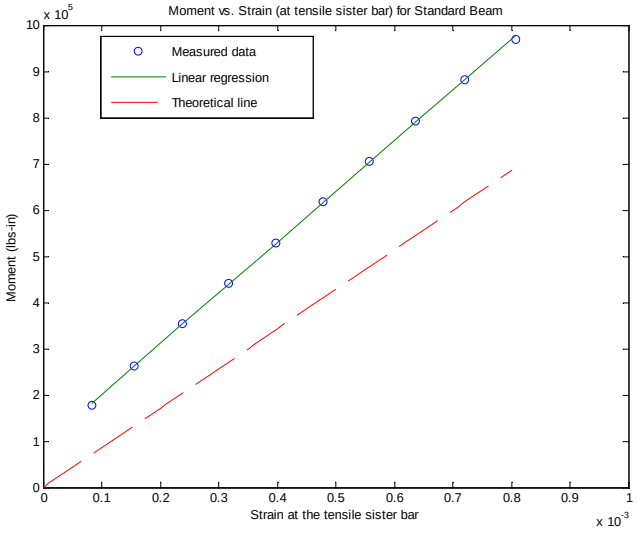

Figure 3.12 Linear Regression for Moment and Strain at Midspan in Tensile Sister Bar for Standard Beam

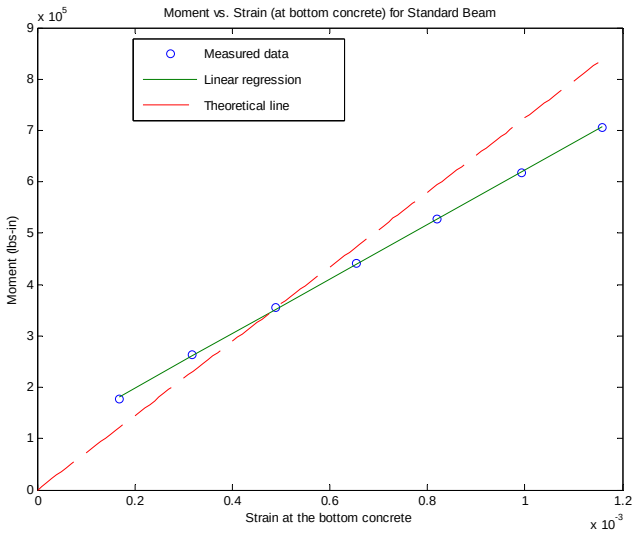

Figure 3.13 Linear Regression for Moment and Strain at Bottom Concrete at Midspan for Standard Beam

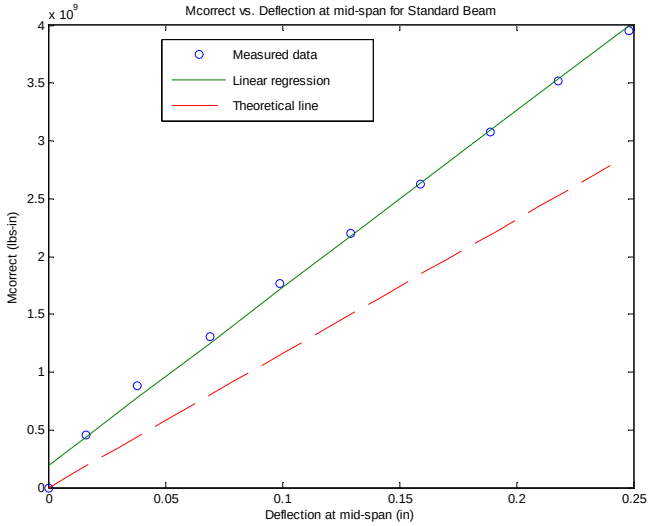

Figure 3.14 Linear Regression for $M_{correct}$ and Deflection at Midspan for Standard Beam

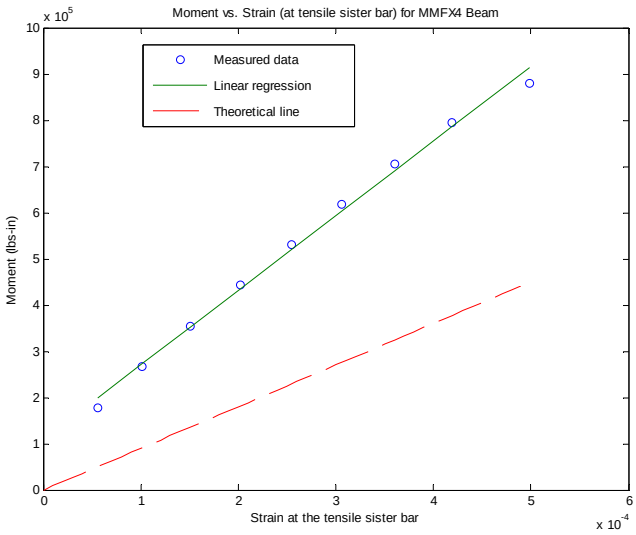

Figure 3.15 Linear Regression for Moment and Strain in Tensile Sister Bar at Midspan for MMFX4 Beam

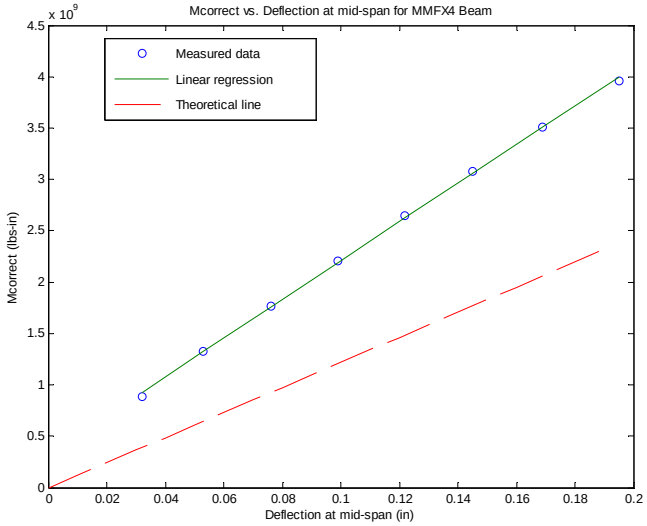

Figure 3.16 Linear Regression for $M_{correct}$ and Deflection at Midspan for MMFX4 Beam

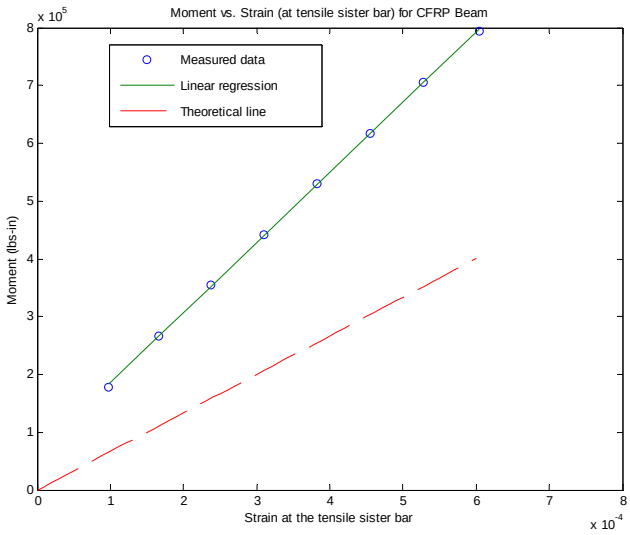

Figure 3.17 Linear Regression for Moment and Microstrain in Tensile Sister Bar at Midspan for CFRP Beam

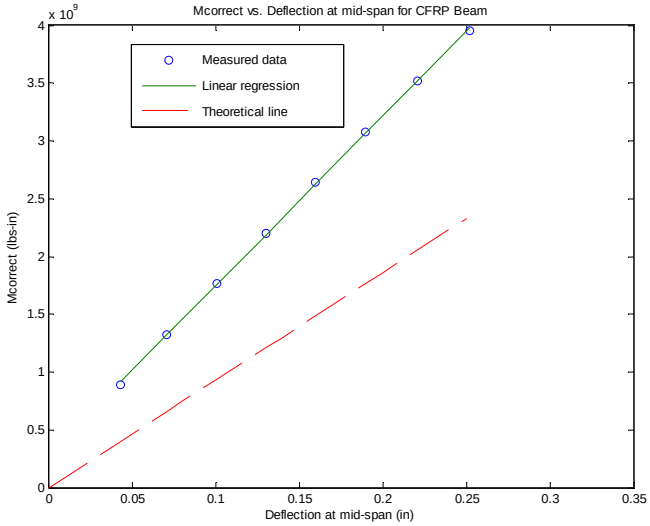

Figure 3.18 Linear Regression for $M_{correct}$ and Deflection at Midspan for CFRP Beam

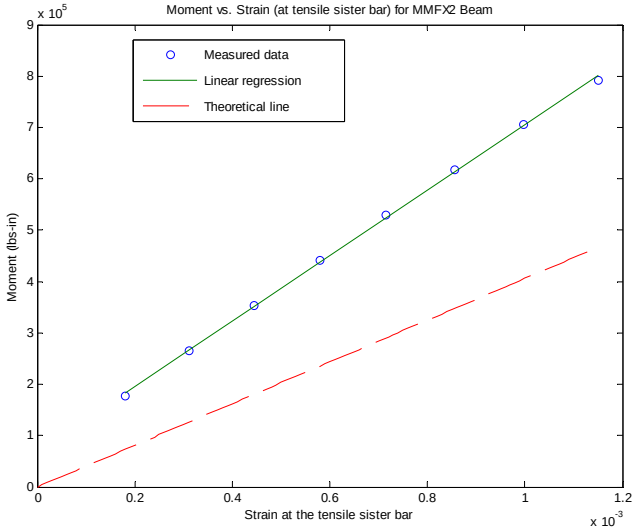

Figure 3.19 Linear Regression for Moment and Strain in Tensile Sister Bar at Midspan for MMFX2 Beam

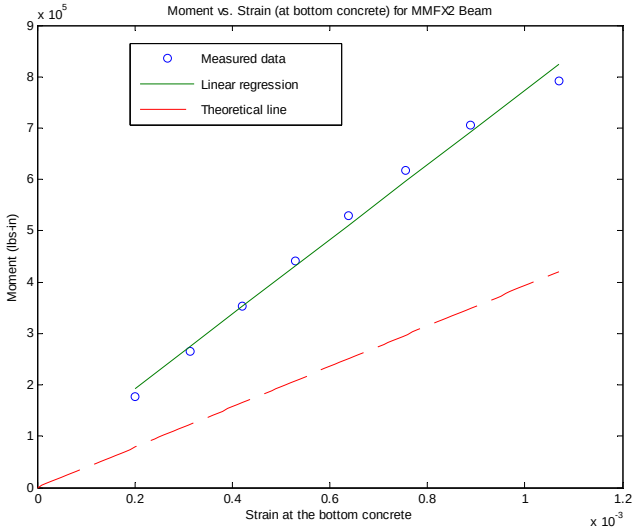

Figure 3.20 Linear Regression for Moment and Strain at Bottom Concrete at Midspan for MMFX2 Beam

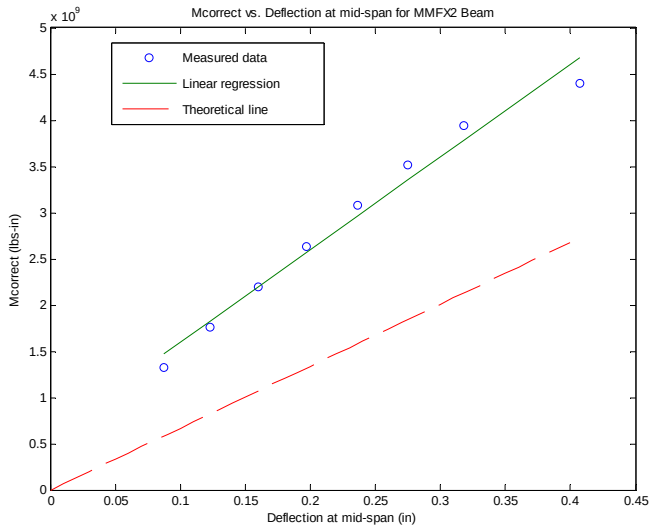

Figure 3.21 Linear Regression for $M_{correct}$ and Deflection at Midspan for MMFX2 Beam

Table 3.4 Theoretical and Measured Moment-Strain Stiffness based on Tensile Steel Strain (Unit: lbs & in)

Test beam	Theoretical $k_{strain} = \frac{M}{\varepsilon_s}$	Measured $k_{strain} = \frac{M}{\varepsilon_s}$	Ratio of measured to theoretical k_{strain}
Standard	8.57×10^8	11.0×10^8	1.28
MMFX4	9.01×10^8	16.7×10^8	1.85
MMFX2	4.06×10^8	6.46×10^8	1.59
CFRP	6.67×10^8	12.1×10^8	1.81

Table 3.5 Theoretical and Measured Moment-Strain Stiffness based on Bottom Concrete Strain (Unit: lbs & in)

Test Beam	Theoretical $k_{strain} = \frac{M}{\varepsilon_{cb}}$	Measured $k_{strain} = \frac{M}{\varepsilon_{cb}}$	Ratio of measured to theoretical k_{strain}
Standard	7.24×10^8	5.31×10^8	0.73
MMFX4	7.61×10^8	N/A	N/A
MMFX2	3.93×10^8	7.78×10^8	1.98
CFRP	5.66×10^8	N/A	N/A

Table 3.6 Theoretical and Measured Moment-Deflection Stiffness (Unit: lbs & in)

Test Beam	Theoretical $k_{defl} = \frac{M_{correct}}{\Delta}$	Measured $k_{defl} = \frac{M_{correct}}{\Delta}$	Ratio of measured to theoretical k_{defl}
Standard	1.16×10^{10}	1.46×10^{10}	1.26
MMFX4	1.22×10^{10}	1.86×10^{10}	1.52
MMFX2	0.67×10^{10}	1.16×10^{10}	1.73
CFRP	0.93×10^{10}	1.47×10^{10}	1.58

Table 3.7 Estimated Steel Area by Steel Strain, Concrete Strain and Displacement (Unit: in^2)

Test Beam	Actual A_s	A_s by steel strain	Percent Error	A_s by concrete strain	Percent Error	A_s by displacement	Percent Error
Standard	1.76	2.27	29%	1.27	-28%	1.41	-20%
MMFX4	1.76	3.22	83%	N/A	N/A	1.74	-1%
CFRP	1.76	3.27	86%	N/A	N/A	1.8	2%
MMFX2	0.88	1.23	40%	1.68	91%	1.22	39%

3.4 Discussion

After studying the collected data and the results of the analysis, the following observations can be made:

1. From the collected data, we see that it is not easy to accurately measure concrete tensile strains using surface mounted BDI transducers, even in the laboratory. This can be partially attributed to local cracking of the concrete. On the other hand, the deflection data measured using the LVDTs looked very good and linearity between the load and deflection is shown in the elastic range (Figure 3.11). From this standpoint, the measured deflection data is more reliable than strain data for concrete members.

2. From Table 3.1, it is observed that the measured cracking moment is much lower than the theoretical cracking moment. For example, for the Standard beam, the theoretical cracking moment is 1.3 times larger than the measured moment. This is consistent with the results obtained by Ashour [Ashour, 2000].

3. From Table 3.7, it is observed that the estimated rebar area based on steel strain is more accurate for the Standard beam than for the MMFX2, MMFX4 and CFRP beams. This may be due to the different bond characteristic for different rebar. It appears that SAM based on measured rebar strain works better for steel rebar than for MMFX and CFRP rebar.

4. It can be observed from Table 3.7 that the estimated rebar area based on concrete strain is more accurate for the Standard beam than for the MMFX2 beam.

5. The estimated area of steel based on measured deflections are reasonably accurate for all four beams (Table 3.7). This proves that SAM based on deflection data works not only for steel rebar, but also for MMFX and CFRP rebar. For example, the error for the Standard beam is around 20% and the error for MMFX4 and CFRP beam is less than 5%.

6. The results of a simple sensitivity analysis for the standard beam are shown in Table 3.8. In this study the area of steel was calculated using an elastic modulus of the concrete equal to 0.8, 0.9, 1.1 and 1.2 times the original assumed value. It shows that the steel areas estimated using strain data are not sensitive to the change of elastic modulus of concrete (E_c). However, it is somewhat sensitive to the assumed elastic modulus of concrete when based on measured deflections.

Table 3.8 Sensitivity Analysis for Standard Beam

Estimated area	E_c	1.1 E_c	Diffe-rence	1.2 E_c	Diffe-rence	0.9 E_c	Diffe-rence	0.8 E_c	Diffe-Rence
By steel Strain	2.27	2.26	0%	2.25	-1%	2.28	0%	2.29	1%
By concrete Strain	1.27	1.26	-1%	1.26	-1%	1.28	1%	1.28	1%
By deflectio n	1.41	1.27	-10%	1.13	-20%	1.57	11%	1.76	25%

7. In summary, laboratory tests confirmed the validity of the Steel Area Method for estimating the area of reinforcing steel in a reinforced concrete beam.

4. Procedure for Load Rating Bridges without Plans by SAM

Using equations (24) and (20), or (31) and (20), in conjunction with data from a diagnostic load test, a slab bridge without plans can be load rated as follows:

1. Instrument the slab with strain gages and/or displacement transducers, concentrating the sensors along the transverse centerline of the slab.

2. Position a loaded vehicle of known weight and axle spacing on the bridge. Record the resulting strains and deflections along with the position of the vehicle.

3. Using the known axle weights and spacing, calculate the moment at the location of the strain measurement using statics, or $M_{correct}$ at the location of the deflection measurement using equation (26).

4. Move the vehicle to a new position and repeat steps 2 and 3. Repeat steps 2 and 3 with the vehicle in a minimum of three different positions (five or more is preferred and will lead to a better estimate of the strain- or displacement-stiffness).

4. Plot the applied moment vs. strain and/or $M_{correct}$ vs. deflection. Fit a linear equation to the data and determine the slope of the best-fit line. Using the slope of the best-fit line and the corresponding equations (24) or (31) determine the location of the neutral axis x.

5. Calculate the estimated area of steel using Equation (20).

6. Carry out a load rating of the slab using the estimated area of steel, using traditional analytical techniques or available rating programs.

5. Verification of the Methodology Based on the Field Test of Bridge 2-063

Though SAM worked well in the laboratory, it still should be validated using a field test before the technique can be applied on a routine basis. The ideal bridge for validating this method would be a simply supported (SS), reinforced concrete slab that is in good condition, has little or no overburden on it, and for which complete structural drawings of the bridge are available.

After searching the Delaware Bridge Inventory, Bridge 2-063 was selected as the best candidate for the test. Bridge 2-063 is a four-span, SS, right (zero skew) bridge with low traffic volume that is in good condition. The bridge is easy to access and easy to set up instrumentation. In the summer of 2004, a diagnostic test was conducted on the bridge to verify SAM.

5.1 Description of the bridge

To test the procedure, a diagnostic load test was conducted on Bridge 2-063, which carries Route 16 over the Marsh Hope Creek in southern Kent County, Delaware. The bridge consists of four SS spans. Only the easternmost span was tested. This span has a clear length of 27’4’’ and an out-to-out width of 49’. It carries two lanes and two shoulders and has integral concrete barriers. The slab is 16.5’’ deep, including a 0.5” wearing surface. The bridge was built in 1958 and is in relatively good condition with no visible large cracks or spalling. A photograph of the bridge is shown in Figure 5.1.

5.2 Test setup and procedure

The bridge was instrumented with strain and displacement transducers. A plan view of the span and the instrumentation layout is shown in Figure 5.2.

BDI strain transducers were mounted along the longitudinal and transverse centerlines of the span. Eleven gages were placed on the transverse centerline, equally spaced at 41.’’ Gages were also mounted on each edge of the deck near the top of the slab. Thirteen gages were placed along the longitudinal centerline, spaced at 43’’ near the center of the span and closer near the supports. The BDI strain transducers have a gage length of three inches and were surface mounted to the slab using a quick setting epoxy. Duplicate strain measurements were made at four locations near the center of the slab. These transducers were fitted with concrete gage extensions to increase the effective gage length to 12 inches. The extensions are recommended if the gages are to be placed over areas where the concrete is believed to be cracked. The regular strain transducers are denoted by a three-digit number. The strain transducers with concrete extensions are denoted by a three-digit number with an “E” on the end.

Figure 5.1 Bridge 2-063, Kent County, Delaware

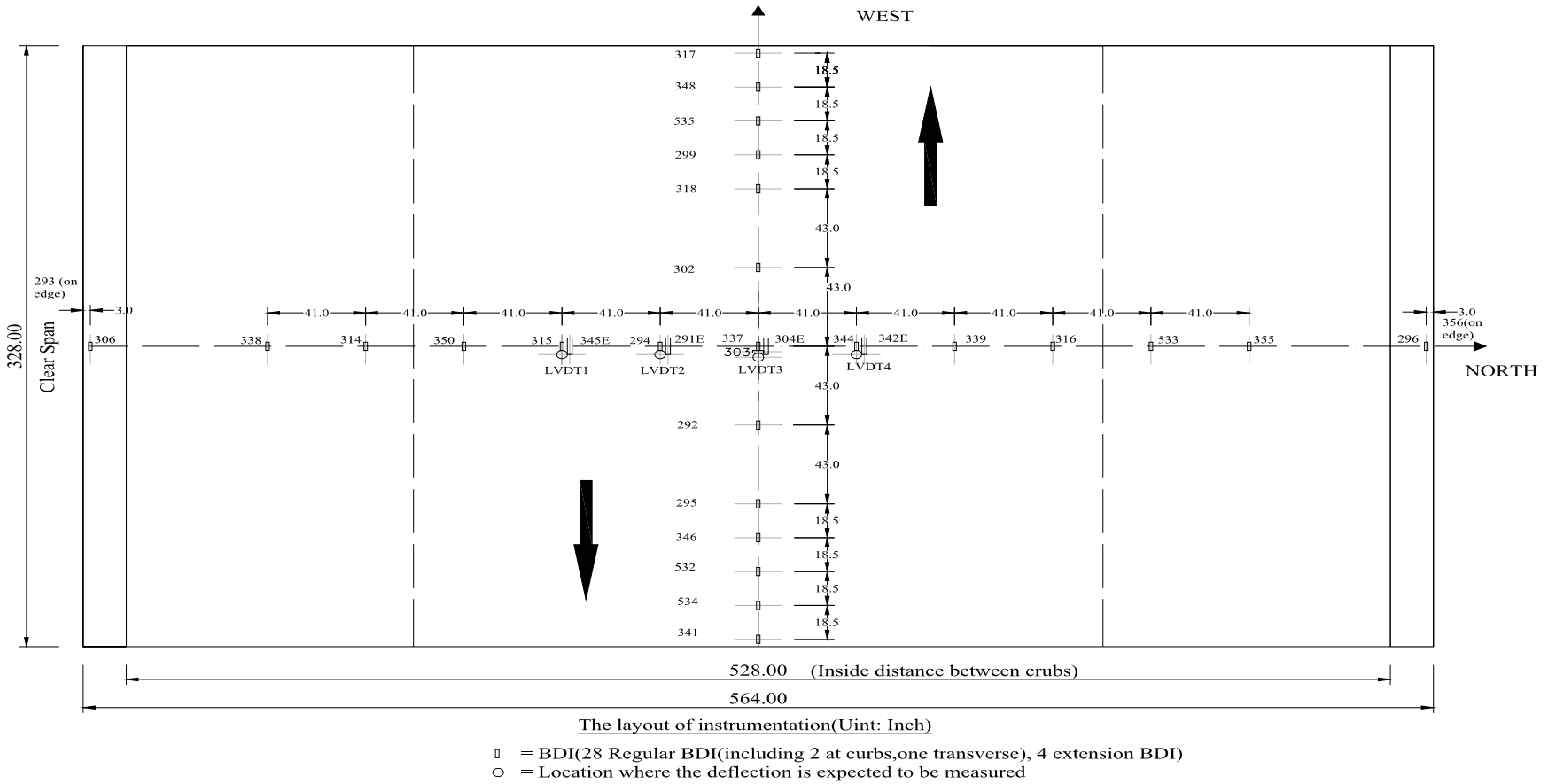

Figure 5.2 Instrumentation Layout

Four LVDT displacement transducers were positioned at midspan to measure the centerline deflection of the slab. The transducers were co-located next to strain transducers, spaced 41'' apart. The displacement transducers have a resolution of 0.001''.

Two loaded ten-wheel dump trucks were used as the controlled load for the test. The plan view of the wheel layout of the trucks is shown in Figure .

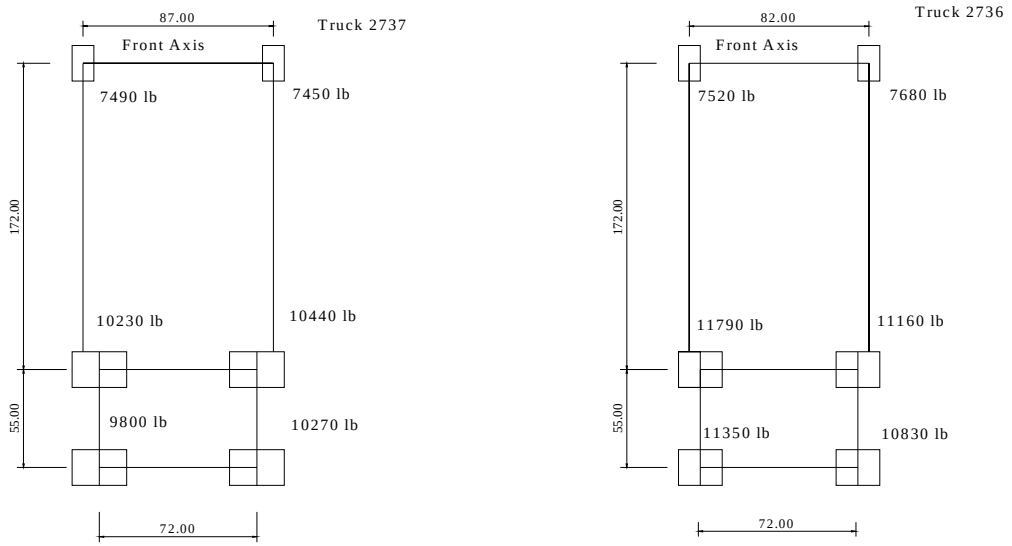

Figure 5.3 Truck Configurations and Weight in Diagnostic Test of Bridge 2-063 (Units: lb & in)

One truck had a gross vehicle weight of 55,680 lbs and the second one a weight of 60,330 lbs. A number of different rolling truck passes were made for the test; however, for this investigation the vehicles were also carefully positioned on the bridge in specific locations and data recorded with the vehicle standing still. The five different static positions of the test truck are shown in Figure 26; the front axle of the rear axle set was placed over the mark and data recorded.

The transverse locations of the tucks for different load paths are shown in Figure 5.5. These transverse locations were involved in eight truck paths, which were designated TS1 to TS8. Among them, TS4 was a repeat test for TS3, which was the truck moving along the centerline of the bridge and was a symmetrical load path. TS8 was a repeat test for TS7, which was two tucks moving side by side in the middle of the traffic lanes and also was a symmetrical load path.

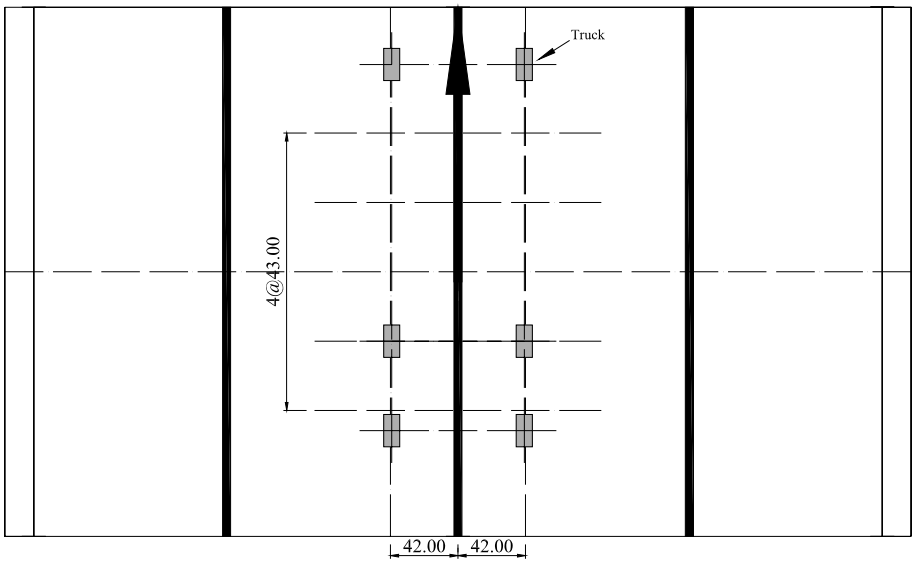

Figure 5.4 Truck Position

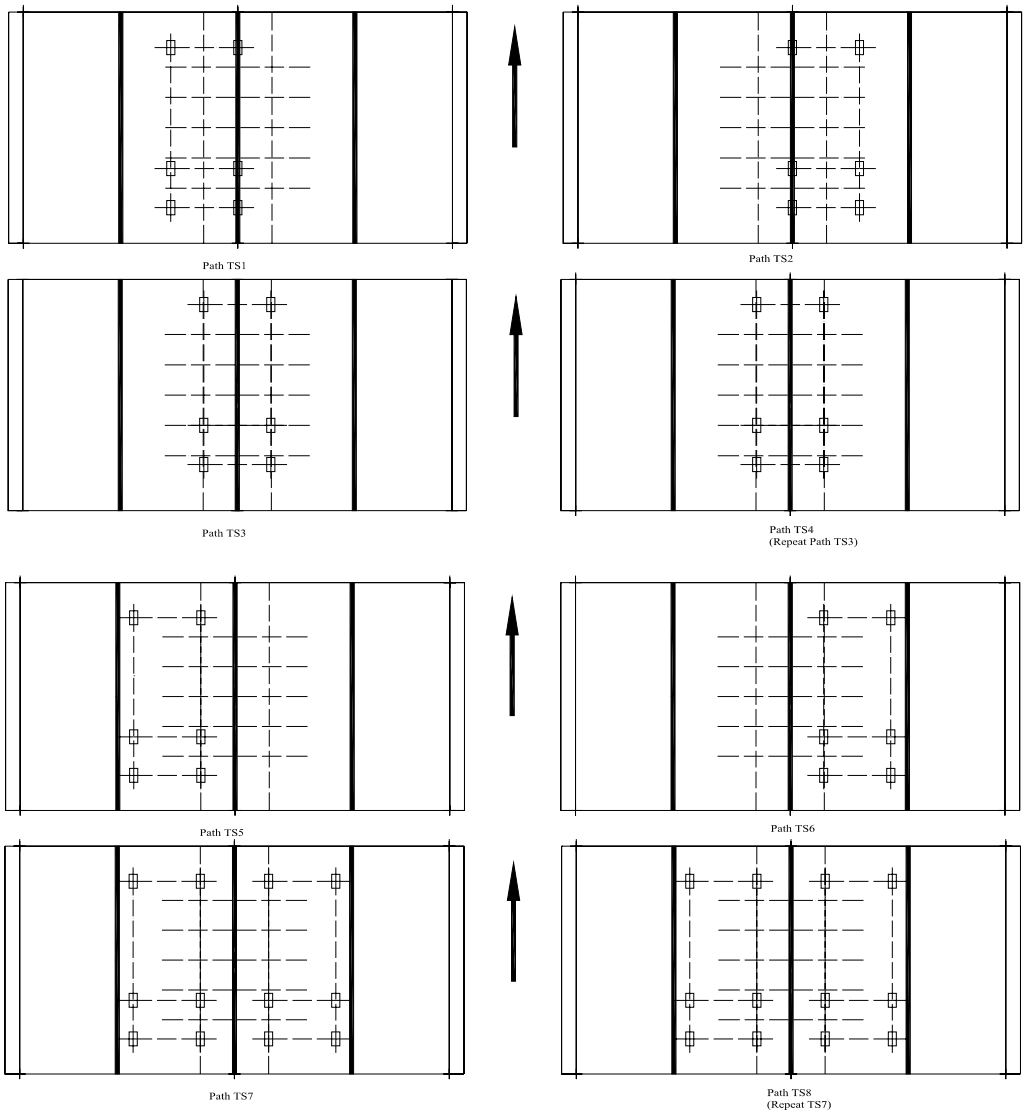

Figure 5.5 Load Passes

5.3 Test Results

In order to determine whether the measured responses are reliable, preliminary data analysis is needed. In this diagnostic test, only concrete strain and displacement were measured. In the preliminary analysis of the data, basic engineering judgment was used to see if the data was reasonable or reliable.

Figure and Figure , which were plotted based on the data recorded from the regular BDI strain transducers (three-inch gage length), illustrated measured strain distribution along the midspan for load paths TS3 and TS7, respectively. TS3 is a symmetrical load path, which was loaded by one truck moving along the centerline. TS7 is also a symmetrical load path, which was loaded by two trucks moving side by side along the center of the traffic lanes. Because the bridge was

designed to be symmetric, engineering judgment says that the strain distributions along midspan for these two load paths are expected to be close to symmetric about the centerline of the bridge. Unfortunately, the results shown in Figure and Figure are not symmetric. Also, because of the symmetry of the structure and loading, the maximum strain response just under the wheels of the trucks should be close. However, big differences are evident in Figure and 29 for the strain response just under the wheels. Furthermore, the values of strain responses recorded in the BDIs located in the central part of the midspan are expected to be close, which cannot be observed from Figure and Figure . Based on these results, it can be concluded that the data recorded by the regular BDIs is not reliable. This supports the comment made earlier based on the laboratory tests that accurate strain measurement for concrete members is difficult even if in the laboratory due to the local cracking of the material, improper setting or limitations of the instrumentation.

The same conclusion can be made from studying the strain history figures. Figure presents the time history recorded by the regular BDIs located in the center part of the midspan for load path TS3. BDI 344 and BDI 294 are two BDIs just placed under the two wheels of the truck. Theoretically, the responses recorded by these two BDIs should be comparable; however, Figure shows large variations for the data recorded by BDI 344 and BDI 294. Checking the time history of gage BDI 337, which was located in between the two wheels of the truck, illustrates there is probably something wrong with BDI 337, for the data recorded by the gage is always close to zero.

On the other hand, the data recorded by the four BDIs with extensions looks better than the regular BDIs. Figure presents the time history for the responses recorded by the four BDIs with extensions in the central part of the midspan in load path TS3. Though the variations among these four BDIs exist, they are not so large and still can be looked as comparable and consistent.

As for the displacement measurements, the data collected looks much better than the strain data. The displacement distribution along midspan is shown in Figure . The trend for this distribution is coincident with the theoretical analysis. The maximum values for the displacement just under the two wheels are very close. The LVDT-3 that was placed in the cross section between the midspan and centerline recorded the maximum response in the test, which was a little bit higher than the maximum values recorded by the LVDTs located just under the wheels. The maximum data recorded by LVDT-1, which was placed outside of the track of the truck began to decrease. The reliability of the data recorded by the LVDTs also can be observed from Figure , which presents the time history of the measured displacement data.

SAM was developed for a beam of width *b*. To apply it to a slab bridge, the bridge must be simplified to a unit beam, which is done using a load distribution factor (DF). The load DF will play a very important role in the later analysis. The problem is we cannot estimate the DF for moment from the measured responses due to the poor quality data recorded by the regular BDIs. Though the BDIs with extension and the LVDT work well, four points are not enough for the DF calculation. Therefore, DFs obtained from finite element analysis (FEA) are used here. The model was setup in the commercial finite element program ANSYS. The Shell 63 element was selected in the analysis. The truck was placed in the model at different transverse locations to simulate the real load paths. The strain distribution along midspan was plotted for each load path

and DF was obtained by the dividing the area under the strain plot by the maximum strain response. The DFs for different load paths are presented in Table 1.

Table 1 Distribution Factors for Wheel Load from FEA

Load path	TS1/TS2	TS3/TS4	TS5/TS6	TS7/TS8
DF	0.058	0.057	0.062	0.10

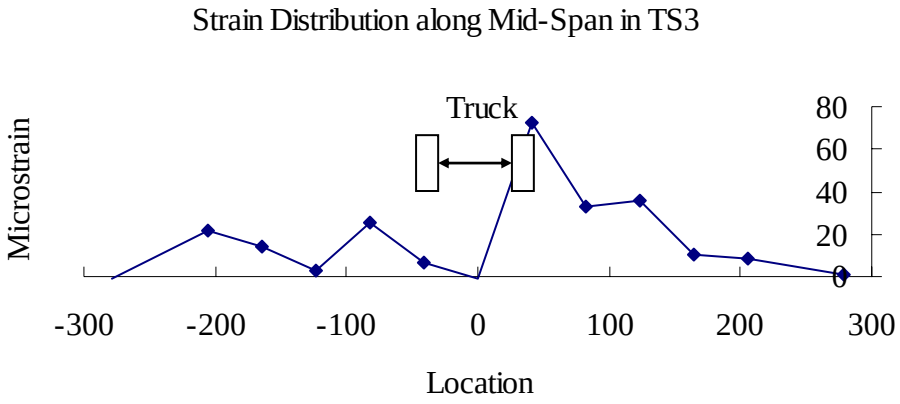

Figure 5.6 Strain Distribution along Midspan in TS3

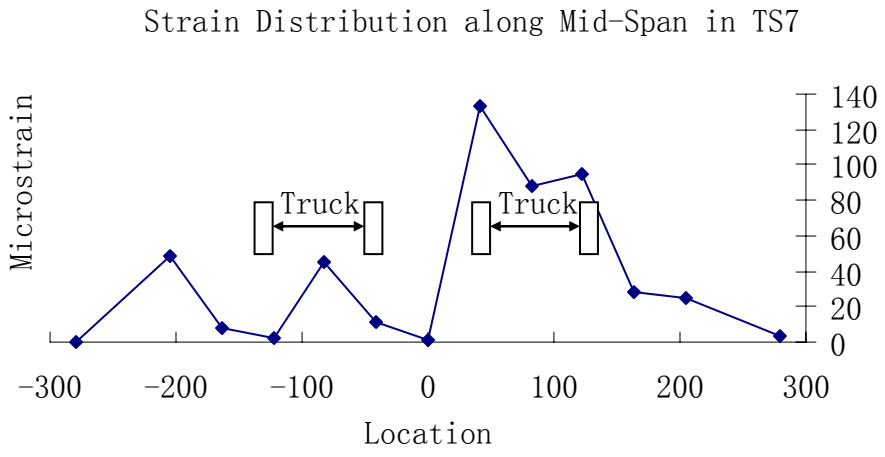

Figure 5.7 Strain Distribution along Midspan in TS7

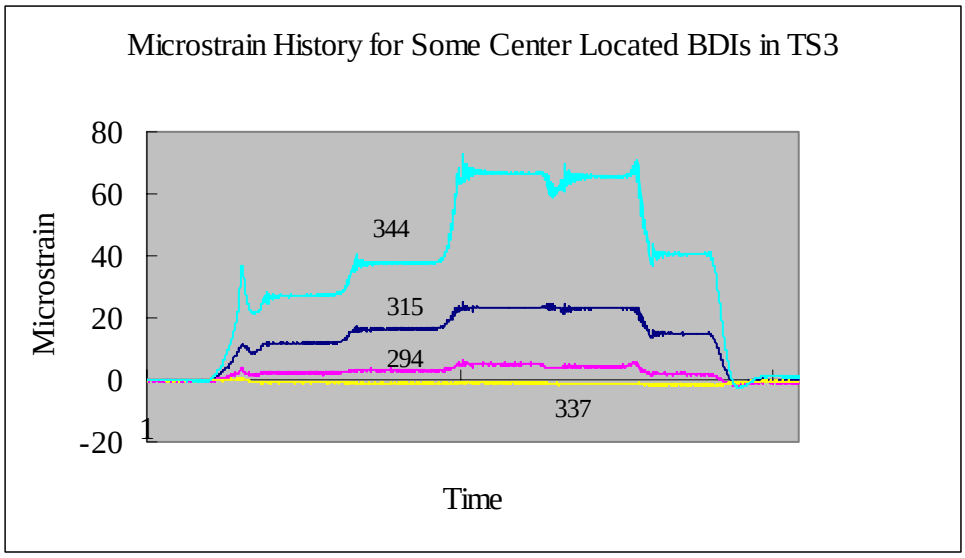

Figure 5.8 Microstrain History for BDI 315/294/337/344 in TS3

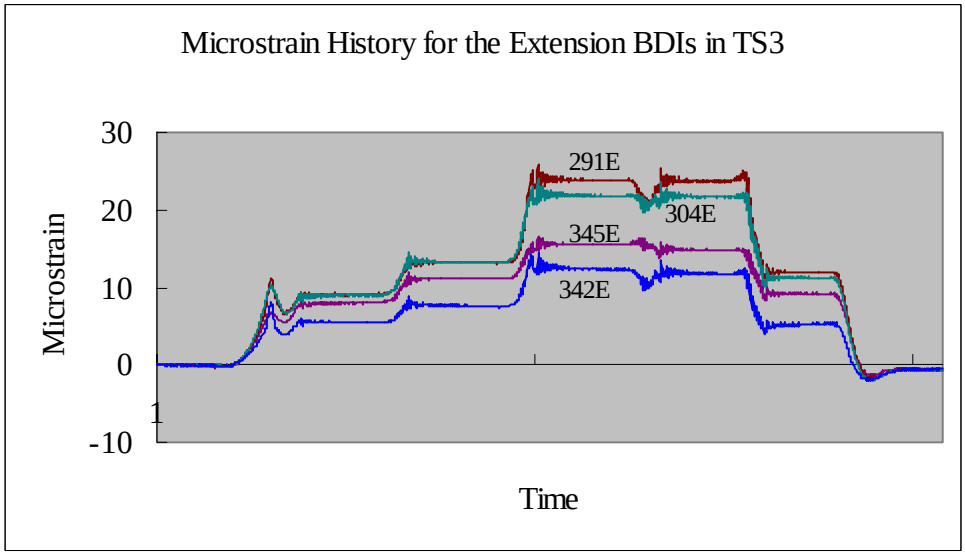

Figure 5.9 Microstrain History for BDIs with 12-in Extension in TS3

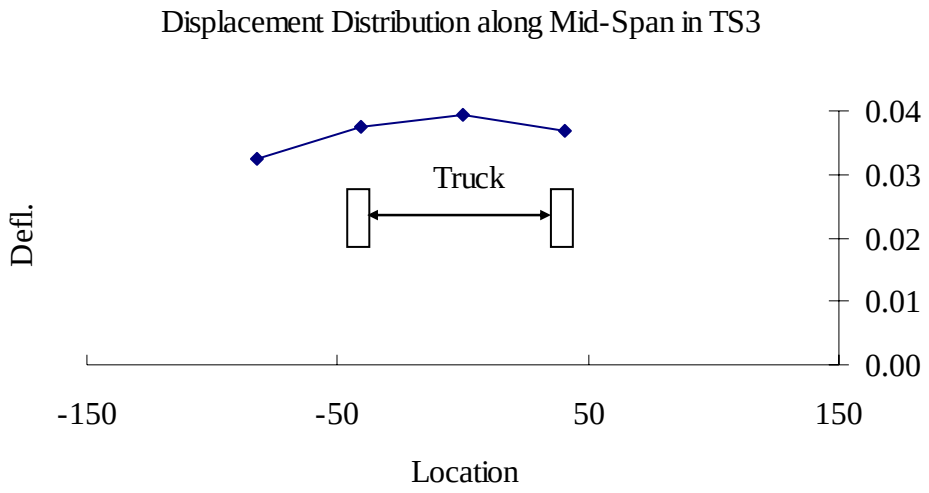

Figure 5.10 Displacement Distribution along Midspan in TS3

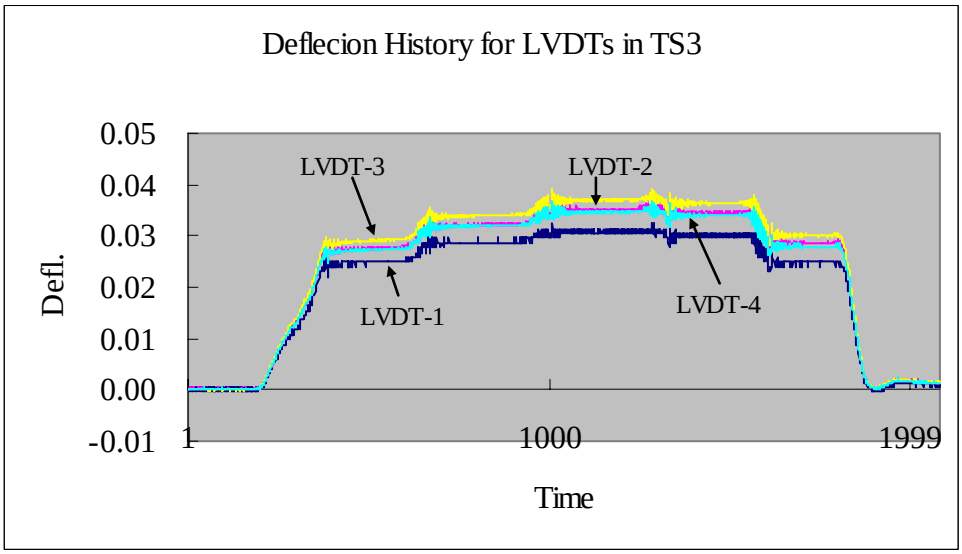

Figure 5.11 Displacement History for LVDTs in TS3

5.4 Steel Area Method Validation

As mentioned previously, we do not have confidence in the data collected from the BDIs gages without extensions; however, the data recorded from the BDIs with extensions and the LVDTs are much more reliable. Therefore, in SAM validation, only the data from the BDIs with extensions and the displacement data are used. The load DFs used in the analysis are computed from the finite element analysis (Table 1).

With regard to the cracking moment, which is used in SAM in terms of the deflection data, tests have shown that equation (28) often overestimates the true cracking moment [Ashour, 2000;

McNally, 2003]. In the following analysis, the cracking moment used is obtained by dividing the value from equation (28) by 1.3, which is ratio of the theoretical cracking moment to the measured one for the Standard beam in the laboratory tests conducted by McNally (see Table 3.1).

The concrete compressive strength was chosen as 10 *ksi*, which is based on Schmidt hammer tests conducted on the slab on the day of the test. The corresponding elastic modulus for concrete is 6063 *ksi*, which is calculated, based on equation 5.4.2.4-1 defined in AASHTO LRFD [AASHTO LRFD, 1998]. The elastic modulus for steel in the analysis is assumed 29000 *ksi*.

Load cases TS3, TS4, TS7 and TS8 are chosen to be used to verify SAM. For each load path, the strain gage that experienced the maximum strain among all the gages, and the displacement transducer that experienced the maximum displacement among all the transducers, was used to determine the moment-strain stiffness and moment-deflection stiffness, respectively. Figure , Figure , 38, and Figure show the linear regression of the moment and strain for BDI 291E at midspan for load path TS3, TS4, TS7, and TS8, respectively. Figure , Figure , Figure , and Figure show the linear regression of $M_{correct}$ and the deflection at midspan for load paths TS3, TS4, TS7, and TS8, respectively. The measured moment-strain stiffness and moment-deflection stiffness and the corresponding estimated steel areas and errors are presented in Table 5.1.

Table

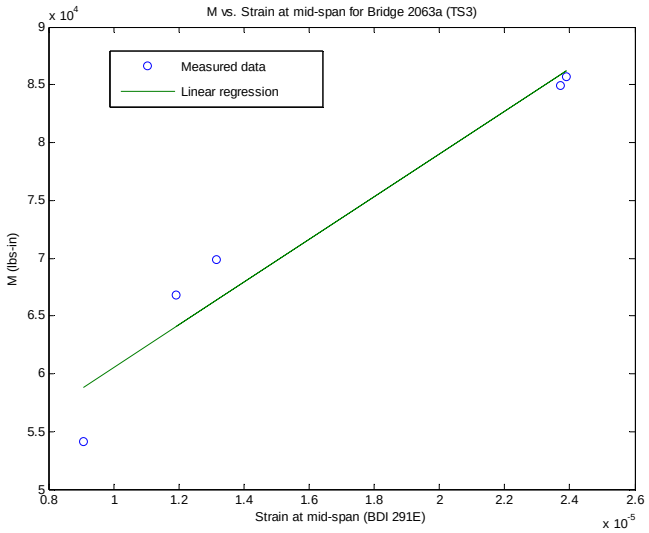

Figure 5.11 Linear Regression for Moment and Strain at BDI 291E at Midspan in TS3

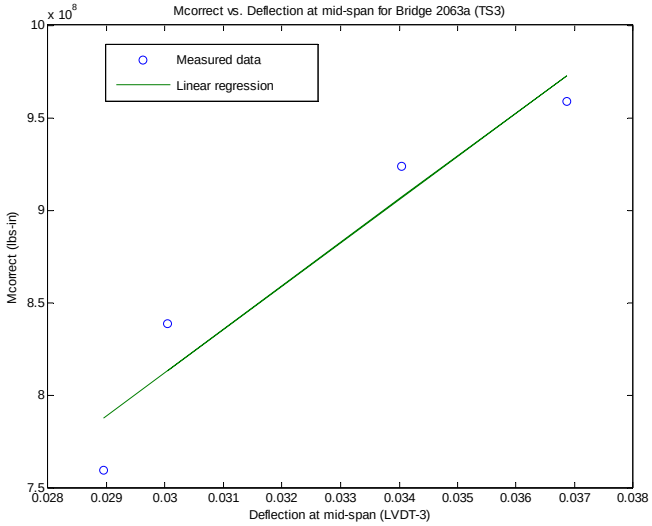

Figure 5.12 Linear Regression for $M_{correct}$ and Deflection at LVDT3 at Midspan in TS3

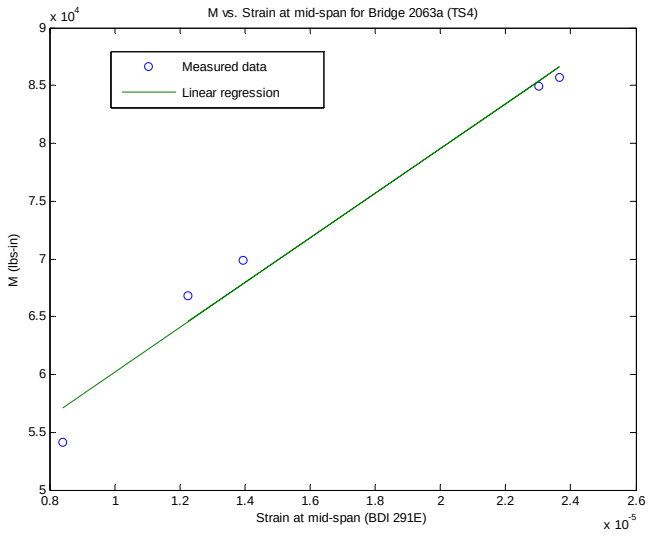

Figure 5.13 Linear Regression for Moment and Strain at BDI 291E at Midspan in TS4

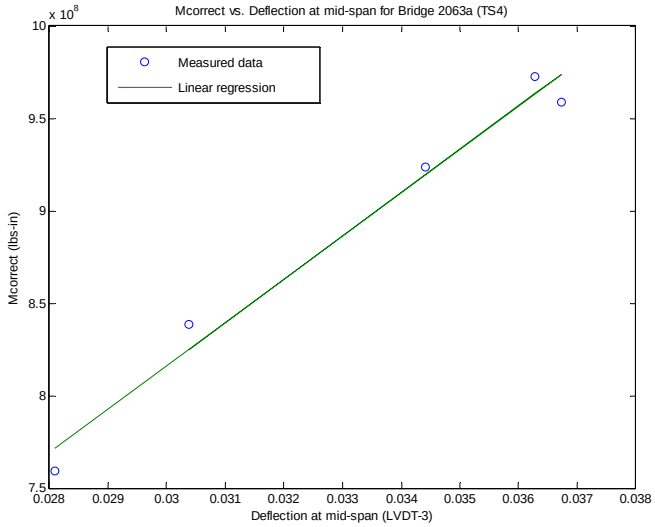

Figure 5.14 Linear Regression for $M_{correct}$ and Deflection at LVDT3 at Midspan in TS4

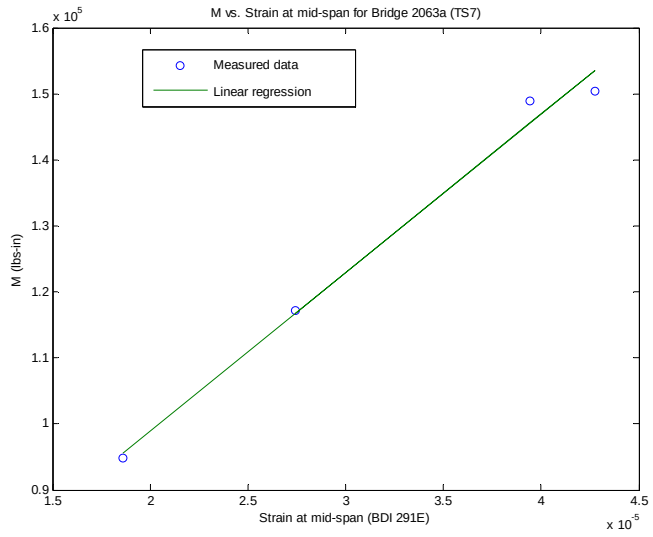

Figure 5.15 Linear Regression for Moment and Strain at BDI 291E at Midspan in TS7

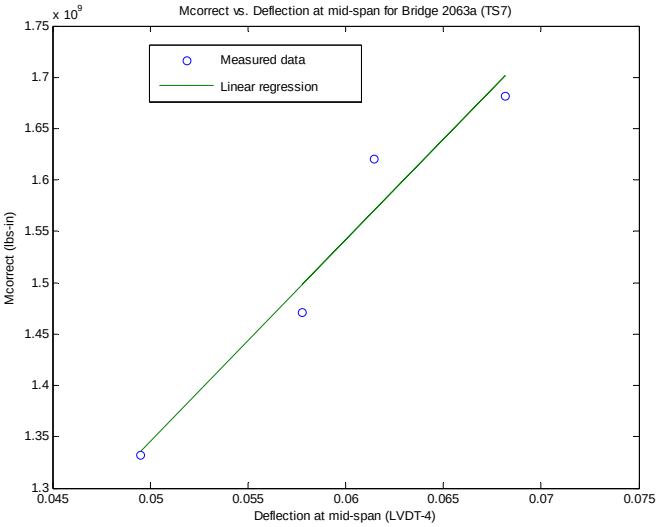

Figure 5.16 Linear Regression for $M_{correct}$ and Deflection at LVDT4 at Midspan in TS7

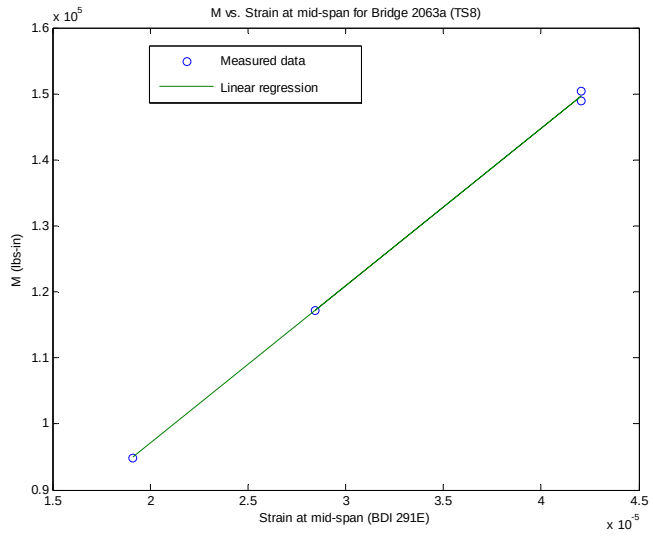

Figure 5.17 Linear Regression for Moment and Strain at BDI 291E at Midspan in TS8

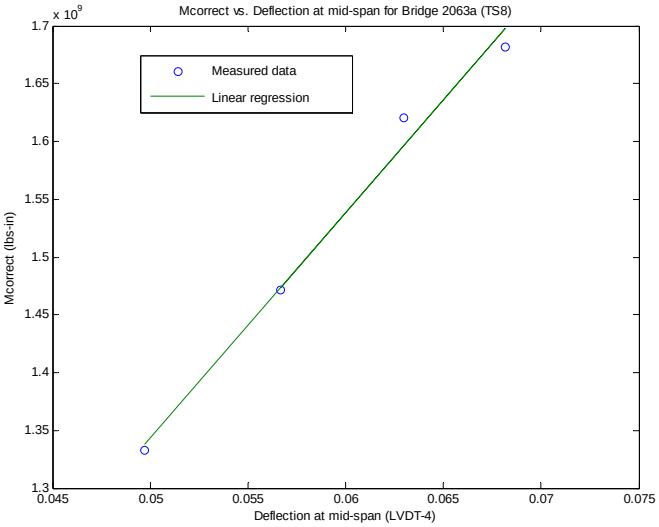

Figure 5.18 Linear Regression for $M_{correct}$ and Deflection at LVDT4 at Midspan in TS8

Table 5.1 Estimated Steel Area by Concrete Strain and Displacement (Unit: lbs & in)

Load Path	Actual A_s	Measured k_{strain}	A_s by k_{strain}	Error	Measured k_{defl}	A_s by k_{defl}	Error
TS3	2.4	1.85E+09	1.41	-41%	2.34E+10	2.80	17%
TS4	2.4	1.93E+09	1.48	-38%	2.34E+10	2.80	17%
TS7	2.4	2.40E+09	1.86	-23%	1.96E+10	3.85	60%
TS8	2.4	2.39E+09	1.86	-23%	1.95E+10	3.77	57%
		Average	1.65	-31%	Average	3.30	38%

5.5 Discussion

Some comments can be made based on the analysis of the test results:

1. By analyzing the transverse strain distribution along the midspan and the time history of the data recorded from the BDI transducers without extensions, it is found that reliable concrete strain measurements using regular BDIs are difficult to obtain. Consequently, the load DFs, which are of crucial importance in simplifying the slab to a unit beam, cannot be estimated from the measured strain data. The DFs used in SAM in this case were obtained from finite element analysis.

2. Compared to the data recorded by the regular BDIs, the data recorded by BDIs with 12" extensions and LVDTs looked much more reliable, especially the displacement data recorded by LVDTs. Though there are only four points in the transverse displacement distribution curve, the trend of this curve is in agreement with engineering judgment and theoretical analysis.

3. Though DFs used in the analysis were not obtained from data recorded by the regular BDIs, it should be possible to estimate the DF using BDIs with extensions or LVDTs, provided there are sufficient transducers of these types spaced correctly along the transverse centerline of the slab.

4. SAM was verified by the diagnostic test done on Bridge 2-063. The estimated steel areas are reasonable, though they are not exactly the same as the actual area due to the assumptions in the model and experimental error. The maximum error was about 60%.

5. In general, the area of steel estimated using the concrete strains recorded by BDIs with 12" extension are less than the actual steel area. This partially may be because those concrete strains are the average over a foot gage length and are not the strain at one point.

6. The area of steel estimated using the displacement data are larger than the actual area. This partially can be attributed to the assumptions made in the developing the method: i.e., modeling the slab as a simple beam, boundary conditions, and secondary member effects.

7. The theoretical cracking moment is usually overestimated. In some cases, the theoretical cracking moment is larger than the moment due to dead load and the test trucks, so the effective

moment of inertia I_e is equal to the gross moment inertia I_g. In that situation, there is no equation available for the neutral axis and thereby no steel area will be estimated. Based on the studies done by other researchers, the cracking moment in the analysis is obtained by dividing the theoretical one by 1.3, which is from the tests done by McNally [McNally, 2003].

8. Pretest analysis and planning is important. Care should be taken in determining the location of the test truck on the bridge to ensure there are enough points in the linear regression process, and to ensure these points have a good distribution in the fitted curve.

5.6 Load Rating Based on the Estimated Steel Area

For load rating concrete bridges without plans, one of the biggest problems is the unknown area of reinforcing steel, which is essential for the calculation of the load-carrying capacity. If the reinforcing rebar information is obtained by SAM, the bridge engineer can follow the same procedure to rate bridges without plans as the ones with plans.

Currently, several commercial programs for load rating bridges are available. One of the most popular programs used in practice is "Bridge Rating and Analysis of Structural Systems" (BRASS), which was developed by the Wyoming Department of Transportation in 1987. The Ultimate Strength Analysis (LFD) portion of BRASS for girders is current with the AASHTO Specifications for Highway Bridges, Fifteenth Edition 1992 with interims [BRASS User Manual, 1996].

The Load Factor Rating method (LFR) is selected herein. The relevant factors for the BRASS load rating input data file are defined in Table . In Table , γ is the load factor for ultimate strength analysis; β_d and β_l are the coefficients for dead load and live load for ultimate strength analysis, respectively; Φ_M is the reduction factor for moment capacity for ultimate strength analysis. The load DF per wheel in the input data file is 0.178, which is computed based on equation 4.6.2.3-2 defined in the AASHTO Specifications [AASHTO LRFD, 1998]. In that equation, L_1 is the modified span length and is taken as 29 *ft* for bridge 2-063; W_1 is the modified edge-to-edge width and is taken as 44 *ft* for bridge 2-063. The equivalent width W per lane is 11.29 *ft* computed from that equation and DF per lane is 0.089 by inverting the corresponding equivalent width. DF per wheel is 0.178, which is obtained by multiplying DF per lane by 2. Bridge 2-063 is assumed as a bridge without plans. The load-rating results at midspan for inventory and operating level based on the actual area of reinforcing steel, the average steel area from concrete strain data, and the average steel area from deflection data are in Table 5.1, are shown in Table 5.3. It is observed in Table 5.3, though the load-rating factors for various rating trucks based on the estimated steel area are not identical to those based on the real steel area, the rating factors based on the estimated steel area are reasonably close to the actual rating factors. Obviously, since the estimated area based on strains is lower than the actual area, the rating factors are lower. Likewise, since the estimated area based on deflections is larger than the actual area, the rating factors are larger. The results presented suggest that the load-rating procedure based on SAM can provide very valuable information about concrete bridges without plans for bridge engineers and owners. For example, if the true steel area of Bridge 2-063 is not

available, the load-rating factors based on the estimated average steel areas at least can provide the lower bound and upper bound for the load rating.

Table 5.2 Factors Defined in the Load Rating

Load Level	γ	β_d	β_l	Φ_M
Inventory Level	1.3	1.0	1.67	0.9
Operating Level	1.3	1.0	1.0	0.9

Table 5.3 Load Rating Results Based on Actual and Estimate Steel Areas at Midspan

Steel area (in^2)		Rating Level	HS20T	S220	S335	S437	T330	T435	T540	Critical
Actual	2.40	IN	1.27	1.83	0.88	0.91	1.71	1.23	1.17	0.88
		OP	2.13	3.06	1.46	1.52	2.86	2.06	1.95	1.46
Average from strain data	1.65	IN	0.74	1.07	0.51	0.53	1.0	0.72	0.68	0.51
		OP	1.24	1.79	0.85	0.88	1.67	1.20	1.14	0.85
Average from deflection data	3.30	IN	1.90	2.72	1.30	1.35	2.55	1.83	1.74	1.30
		OP	3.17	4.55	2.18	2.26	4.26	3.07	2.91	2.18

5.7 Load Rating Based on the Simplified Method

For comparison, the simplified method (SM) will be used to load rate bridge 2-063 based on the diagnostic load test results in this section. The allowable stresses in the inventory level and operating level for the reinforcing rebar are assumed 20 *ksi* and 28 *ksi* for the unknown grade after 1954, respectively, according to the AASHTO Manual for Condition Evaluation of Bridges [AASHTO, 1994]. The Young's modulus for the reinforcing rebar E_s is assumed 29000 *ksi*. Therefore, the allowable microstrain in the reinforcing steel at the inventory level is

$$\varepsilon_{all} = \frac{20}{E_s} \times 10^6 = 690\ \mu\varepsilon$$

The allowable microstrain in the reinforcing steel at the operating level is

$$\varepsilon_{all} = \frac{28}{E_s} \times 10^6 = 966\ \mu\varepsilon$$

In the diagnostic test, the maximum measured microstrain at midspan was 42.75, which was recorded in TS7. The corresponding moment due to the test trucks is 1.5×10^5 *lbs-in*, which is

based on DF in Table 1. Assuming the concrete density is 150 $lbs/\ ft^3$, the moment due to dead load at midspan for the unit wide SS beam is 2.6×10^5 *lbs-in*. Conservatively assuming both the live load and dead load are acting on the cracked section, the concrete microstrain due to dead load ε_{DL} can be estimated if the linear relationship between moment and strain holds,

$$\varepsilon_{DL}=\frac{2.6\times10^5}{1.5\times10^5}\times42.75=74.1\mu\varepsilon$$

Though the steel strain will be less than the concrete strain, since the distance from the rebar to the bottom of the beam is relatively small, the steel strain due to dead load can be conservatively estimated to be equal to the concrete strain.

The theoretical moments plus impact factor at midspan due to the various rating trucks undertaken by the unit beam are listed in the fourth row in5.4. The AASHTO specified load distribution 0.178 is used in the calculation of the theoretical moments. Following the same idea as the dead load strain estimation, the concrete or steel microstrain due to various rating trucks are computed and listed in the sixth row in5.4. Herein, the impact factor is chosen as 0.3. The rating factors for various rating trucks based on SM are shown in the last two rows in Table 5.4 at inventory level and operating level, respectively. It is observed that the rating factors based on SM are improved, compared to the theoretical rating factors in Table 5.3. The improvement can be attributed to the fact that the in-situ information, such as the actual material properties, boundary conditions, and secondary member effects, are included in the SM load-rating results. The advantage of SM is its simplicity, for example, no reinforcing steel area is needed in the calculation. Though it is an approximate technique, it can still provide engineers a simple way to evaluate the load-carrying capacity based on the diagnostic load test. It should be noted, however, that the measured strain in diagnostic test was used to estimate the responses under dead load or rating trucks, the bridge is assumed to work linearly and in its elastic limit even if under the load level which are bigger than the test trucks.

Table 5.4 Load Rating Results Based on SM at Midspan (Unit: $\mu\varepsilon$; lbs & in)

	HS20T	S220	S335	S437	T330	T435	T540
ε_{all} (IN)	690	690	690	690	690	690	690
ε_{all} (OP)	966	966	966	966	966	966	966
ε_{DL}	74.1	74.1	74.1	74.1	74.1	74.1	74.1
$M_{LL}(1+I)$	3.3×10^5	2.3×10^5	4.8×10^5	4.7×10^5	2.5×10^5	3.4×10^5	3.6×10^5
ε_{LL}	94.4	65.9	137.3	132.7	70.3	97.6	103.1
RF (IN)	6.5	9.3	4.5	4.6	8.8	6.3	6.0
RF (OP)	9.1	13.0	6.3	6.4	12.3	8.8	8.4

6. Summary

Load rating bridges without plans is a difficult problem that bridge engineers and owners have to face, especially for concrete bridges without plans. The Steel Area Method (SAM) and the Simplified Method (SM), which incorporates the results of a diagnostic load test, have been developed to address this problem. The main work and conclusions of this study are presented below.

Equations have been extended for estimating the area of reinforcing steel in a beam or slab based on measured strains or deflections, for very general load cases. This is particularly important when the load used in the field test is a mulit-axle vehicle. By measuring the moment-strain stiffness or the moment-deflection stiffness, the neutral axis of the member and the area of steel can be estimated.

Laboratory tests on four beams have been used to validate the SAM. For each beam, reinforcing steel area was estimated using the measured (1) tensile strain in the rebar, (2) concrete strain on the bottom of the beam (if applicable) and (3) beam deflection. Based on the test results, some observations can be made:

- The displacements measured in the test are more reliable than the concrete strains measured on the bottom of the beam. This is because the strains are affected by local cracking in the region of the strain gage.

- The cracking moments estimated based on theory are higher than the actual cracking moments measured in the tests, by about 30%. This has an effect on the area of steel estimated using the SAM.

- Provided the measured strain or deflection data is of sufficient quality, the SAM can provide a reasonable estimate of the area of reinforcing steel in the beam.

A procedure for load rating bridges without plans based on SAM was proposed and verified by the field test on Bridge 2-063 whose plans are available. The procedure uses a controlled diagnostic load test to estimate the area of reinforcing steel in the concrete slab. Once the area of steel is estimated, the slab can be rated using traditional techniques. Based on the results of this investigation, the following conclusions can be stated:

- The displacement data obtained from the LVDTs and the strain data obtained from the BDIs with extensions in the controlled diagnostic test were more reliable and consistent than the concrete strain data obtained from the BDI transducers without extensions. In future tests of concrete slabs, BDI transducers should be used only with extensions.

- SAM was verified based on the diagnostic test of Bridge 2-063. The estimated steel areas are reasonable though they are not exactly the same as the actual area. The errors can be attributed to the assumptions in the model and measurement error. In general, the area of steel estimated based on the concrete strains recorded using BDI gages with extensions are less than the actual steel area. The area of steel estimated based on the measured

deflections are greater than the actual area. It is recommended that when possible both strains and deflections be measured in the test and independent estimates of the area of steel be made. The actual area is likely to between the two estimates.

- Because of the poor data obtained from the BDI gages without extensions, the measured load distribution factors were not available: therefore, the load distribution factors computed from finite element models were used in the procedure verification. The procedure developed is very sensitive to the distribution factor used in the analysis. In the future, the test setup should include at least six sensors (displacement transducers and/or BDI strain sensors with concrete extensions) spaced along the transverse centerline of the slab, so that the distribution factor can be obtained from the test results.

- Although the load-rating factors for various rating trucks based on the estimated steel area are not identical to those based on the actual steel area, they are reasonable. The load-rating procedure based on SAM can provide very valuable information about concrete bridges without plans for bridge engineers and owners.

Rating factors based on the simplified method are improved (i.e., larger), compared to the load rating factors obtained from the purely theoretical analysis. The improvement can be attributed to the fact that the in-situ information is included in the load-rating results through the simplified method. Though it is an approximate technique, it still can provide engineers a simple way to evaluate the load-carrying capacity based on the diagnostic load tests. However, the engineers have to be cautious about the application of the simplified method when the diagnostic load test results are used to extrapolate the bridge response to higher load levels than the test trucks. Where possible, both the SAM and SM methods should be used to arrive at a new load rating for the bridge.

References

AASHTO Manual for Condition Evaluation of Bridges, Washington, D.C., 1994.

AASHTO, LRFD Bridge Design Specifications, Washington, D.C., 1998.

ACI 440.1R-01, "Guide for the Design and Construction of Concrete Reinforced with FRP Bars," Reported by ACI Committee 440, Michigan, 2001.

Ashour, S.A., "Effect of Compressive Strength and Tensile Reinforcement Ratio on Flexural Behavior of High-Strength Concrete Beams," Engineering Structures, 22, pp. 413-423, 2000.

BRASS-Girder User Manual, Version 5, Wyoming Department of Transportation, 1996.

McNally, M.M., "Behavior of Reinforced Concrete Beams Designed with MMFX and CFRP Rebar," Master's Thesis, University of Delaware, 2003.

Thompson, E., "Evaluation the Load Carrying Capacity of Bridges without Plans Using Field Test Results," Master's Thesis, University of Delaware, 1999.

Delaware Center for Transportation
University of Delaware
Newark, Delaware 19716